Endothelial-to-mesenchymal transition in Dupuytren’s disease

Sturhahn, Leon

UNIVERSITY OF SPLIT

SCHOOL OF MEDICINE

Leon Sturhahn

ENDOTHELIAL-TO-MESENCHYMAL TRANSITION IN DUPUYTREN'S DISEASE

Diploma thesis

Academic year:

2023/2024

Mentor:

Marin Ogorevc, MD, PhD

Split, July 2024

TABLE OF CONTENTS

ACKNOWLEDGEMENT

First and foremost I have to express my deepest gratitude to Marin Ogorevc, MD, PhD, who has been a better mentor than I ever could have imagined and a friend who has embodied the spirit of what I love about Split. You have been exceptional in every way I could have wished for.

I am also deeply appreciative of my family for their guidance when I felt lost and for their support in ways I did not even know I needed. You have helped me believe my dreams are achievable. My gratitude extends to my chosen family; your presence made what at times seemed overwhelming truly enjoyable.

Lisa and Fabi, I am so grateful for you contributing to who I am. You have given me so much more than just the time we spent together.

Finally, thank you Santi. You are everything I have always hoped for but never expected to find.

LIST OF ABBREVIATIONS

αSMA – α-smooth muscle actin

BMP – bone morphogenetic protein

CA – central aponeurosis

CTGF – connective tissue growth factor

DD – Dupuytren‘s disease

EndoMT – endothelial-to-mesenchymal transition

EMT – epithelial-to-mesenchymal transition

ECM – extracellular matrix

FGF – fibroblast growth factor

FGFR1 – fibroblast growth factor receptor 1

IL – interleukin

LDS – lateral digital sheet

MET – mesenchymal-to-epithelial transition

MCP – metacarpophalangeal

NL – natatory ligament

PNF – percutaneous needle fasciectomy

PIP – proximal interphalangeal

TF – transcription factor

TGF-β – transforming growth factor beta

TLPF – transverse ligament of the palmar fascia

TWIST – twist-related protein

VEGF – vascular endothelial growth factor

ZEB – zinc-finger e-box binding homeobox protein

1. INTRODUCTION

1.1. Anatomy of the palmar fascia

The palmar fascial complex of the hand comprises five components: the palmodigital fascia, digital fascia and the radial, ulnar and central aponeuroses (1). Dupuytren's disease (DD) primarily affects the central aponeurosis (CA), a triangular fascial layer with longitudinal, transverse, and vertical fibers. The longitudinal fibers of the CA extend into three bands for the central digits, each band branching distally. These fibers insert in three layers: superficially into the dermis, intermediately as the spiral band, and deeply near the extensor tendon (2). Transverse fibers of the CA comprise the natatory ligament (NL) and the transverse ligament of the palmar fascia (TLPF). The TLPF, located proximal and parallel to the NL and below the pretendinous bands, forms the septa of Legueu and Juvara, which protect neurovascular structures and provide support to flexor tendons (1). Vertical fibers of the CA form bands connecting the palmar fascia to the skin and create fibroosseous compartments. These eight vertical septa divide the hand into seven compartments: four containing flexor tendons and three containing common digital nerves, lumbrical muscles and arteries (3).

In the interdigital folds, additional fascial structures include the spiral band and the NL (4). The spiral band originates as the middle layer of a bifurcated pretendinous band, spiraling towards the palm's center, and then courses distally perpendicular to the palm, ending near the metacarpophalangeal (MCP) joint capsule. It connects the palmar and digital fascial structures. The NL fibers run transversely but form a U shape distally, aligning longitudinally along adjacent digits towards the lateral digital sheet (LDS). The NL extends to the first web space as the distal commissural ligament. The LDS receives contributions from both the spiral band and the NL (4). In the digit, the neurovascular bundle is enclosed by four fascial structures: Grayson’s ligament palmarly, Cleland’s ligaments dorsally, the LDS laterally, and potentially a retrovascular fascia medially and dorsally, although its existence is debated (5).

1.2. Dupuytren’s disease

DD, also known as Dupuytren's contracture, is a benign fibroproliferative disorder primarily affecting the ulnar aspect of the palmar fascia, with development of fibrotic cords, potentially leading to progressive flexion contractures and deficits in extension across MCP and interphalangeal joints (6). While the formation of nodules commonly precedes the development of cords, cords can also form independently. Both nodules and cords are pathognomonic of DD (7). Patients initially often notice changes in the skin of the palm,

including reduced flexibility or elasticity (8). Early joint contracture is a result of the progressive shortening of the cords, which are in digital, palmar or palmodigital regions. In advanced stages, capsuloligamentous tissue scarring may contribute to the formation of joint contracture (9). Disease progression, while not universal, commonly results in flexion deformities, particularly in the MCP and proximal interphalangeal (PIP) joints of the fourth and fifth digits (10). Other digits may also be affected, with the thumb typically being the last to show involvement. Although spontaneous regression is possible, DD can significantly impact hand functionality, adversely affecting patients' quality of life (11).

1.2.1. Epidemiology

DD presents with a mean prevalence of 8.2% worldwide. The highest prevalence rate is found in Africa at around 17%, followed by 15% in Asia and 10% in Europe, while North and South America have a prevalence of 2% (12). The heterogeneity of the epidemiological studies on DD may partially be attributed to the scarcity of included studies from Africa and the nomenclature which inconsistently differentiates between DD and Dupuytren's contracture (13). A notable sex dimorphism exists in DD, with males showing a three to four times higher incidence and a predilection for severe manifestations, potentially linked to the expression of androgen receptors in Dupuytren fascia (14). DD is particularly rare in the younger population. The incidence of the disease per 10,000 individuals increases with age, rising from approximately 5 in those under 50 years of age to 15 in the 50–59 age group, 30 in the 60–69 age group, and 40 in those aged 70 or older (13). By the age of 90, incidence in the sexes becomes equal (15).

1.2.2. Etiology

To properly discuss the etiology of palmar fascial disorders, it is essential to distinguish between typical DD and Non-Dupuytren's palmar fascial disease. Typical DD frequently affects Caucasian males of Celtic or Scandinavian origin, with a mean onset age of around 57 years, bilateral involvement and a progressive course. Ectopic manifestations in typical DD are not uncommon. Family history is typically positive among these patients, indicating a genetic predisposition (16). In contrast, Non-Dupuytren's palmar fascial disease is characterized by a lack of family history, affects a more ethnically diverse population, and has no gender predilection. It typically manifests unilaterally, without ectopic manifestations, and tends to be nonprogressive or regressive, therefore, surgery is rarely indicated. The disease usually presents as a localized or diffuse thickening of the palmar fascia. Environmental factors such as trauma or previous hand surgeries may play a role in

its development (17). DD demonstrates a heritability of approximately 80%, substantiated by twin and genomic studies identifying 85 genome-wide significant single nucleotide polymorphisms across 56 associated loci (8, 18). Additionally, DD exhibits varying degrees of association with conditions such as plantar fibromatosis (Ledderhose disease), Peyronie's disease, type 1 and type 2 diabetes mellitus, hepatic disorders, and epilepsy (19). Age represents a consistent risk factor, while occupational exposure to vibrating instruments for durations exceeding 15 years has been significantly correlated with DD development (20). Modifiable lifestyle factors, such as tobacco use and alcohol consumption, further elevate disease prevalence in a dose-dependent relationship (21). While the influence of smoking has heavily been debated in the literature, the impact of alcohol on DD development is believed to be multifactorial, including increased oxidative stress, increased production of transforming growth factor beta (TGF-β), and the interference of ethanol intoxication with collagen synthesis (22-24). Contrary to earlier hypotheses, genetic analyses have refuted any specific association between Nordic ancestry and DD (25).

1.2.3. Pathogenesis

The genetic influence on DD is considered predisposing rather than causative (26). One hypothesis is that individuals with a genetic predisposition experience additional events leading to local microvascular ischemia and the formation of free radicals (14). However, Bayat *et al*. reported a maternally inherited pattern of Dupuytren's disease, revealing a mutation in the mitochondrial genome in 90% of these patients. These defective mitochondria produce highly elevated levels of free radicals and exhibit impaired apoptotic mechanisms, thereby directly contributing to the disease pathology (27). There is evidence linking DD with advanced age, male sex, positive family history of Dupuytren's disease, and diabetes mellitus. Furthermore, heavy alcohol drinking, cigarette smoking, and manual work with vibrating tools exposure show a significant dose-response relationship with DD (28). The male predominance in DD is associated with androgen receptor expression in the Dupuytren's fascia rather than genetic factors (29). Trauma, such as typical hyperextension injuries can lead to micro ruptures in the palmar fascia, which will generate a repair process that involves the generation of interleukin (IL) 1, the most abundant cytokine in DD-affected fascia (30). IL-1 stimulates platelets and macrophages to produce growth factors such as TGF-β, the most abundant growth factor in DD fascia (31), causing differentiation of fibroblasts into myofibroblasts, increased extracellular matrix (ECM) component

production, selective fibronectin splicing and platelet activation (**Figure 1**). Furthermore, in vitro studies showed IL-1 causing direct fibroblast proliferation as well as epidermal Langerhans cell stimulation, causing their migration to the dermo-epidermal junction and Dupuytren‘s nodules (32). The extrinsic theory of DD states that these stimulated Langerhans cell will initiate the events that lead to contracture (33). Another potential pathway linking trauma to DD development involves injury distal to the elbow, causing ipsilateral vasomotor disturbance and secondary ischemia of the palmar fascia. This is supported by industrial workers developing DD after limb injuries with concurrent reflex sympathetic dystrophy (34). Further evidence of microangiopathy in DD includes narrowed microvessels and their thickened basal laminae. Ischemia converts adenosine triphosphate to hypoxanthine and xanthine dehydrogenase to xanthine oxidase. Xanthine oxidase then catalyzes the oxidation of hypoxanthine to xanthine and uric acid, releasing free radicals (35). Alcohol consumption is also associated with increased conversion of xanthine dehydrogenase to xanthine oxidase (36). Elevated levels of free radicals have been shown to cause an increase in fibroblast density in the cord and nodular areas of the DD-affected palmar fascia (35). Finally, antioxidant enzyme activities decrease with age in fibroblasts, hence aging acts by both vascular and metabolic mechanisms (27). In DD-affected fascia, there is excessive collagen production, particularly of type III Collagen (37). This excessive type III collagen production is not due to a genetic defect in collagen production but secondary to increased fibroblast density (38). Other contributing factors include the stimulation of fibroblasts by growth factors, decreased fibroblast apoptosis and an imbalance of collagenases and their inhibitors (39). Ultimately, myofibroblasts are the main responsible cells for the contractile force in DD. Intracellular actin filaments are continuous through the cell membrane with extracellular fibronectin fibrils, which in turn connect with extracellular collagen bundles. The fibronexus, present at the cell membrane, interconnects actin microfilaments and fibronectin fibrils. When myosin is activated, the contractile force from the intracellular actin microfilaments is transferred to the extracellular collagen bundles, leading to progressive contracture of the DD-affected fascia (40). This hypothesis is supported by the temporal association between the emergence of a densely cellular nodule, characterized by randomly oriented spindle-shaped fibroblasts with increased α-smooth muscle actin (αSMA) expression, and the alignment of these cells along lines of tension at the onset of contracture (41).

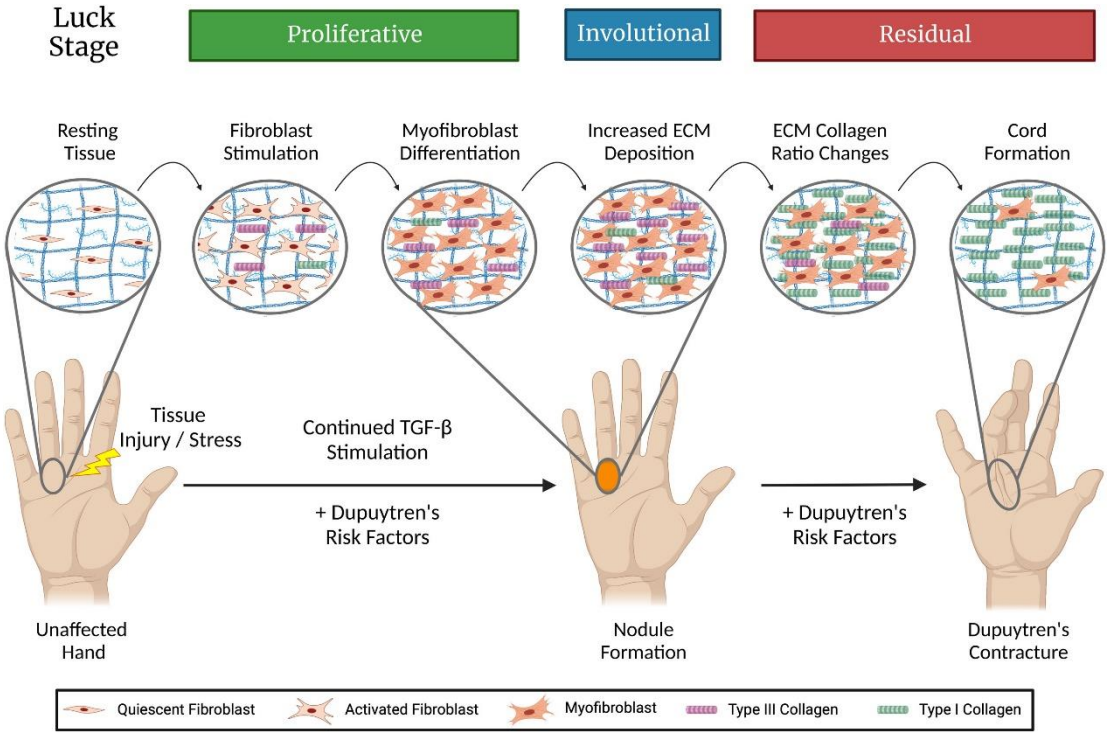

Figure 1. Pathogenesis of Dupuytren's disease. Source: Lambi AG, Popoff SN, Benhaim P, Barbe MF. Pharmacotherapies in Dupuytren disease: current and novel strategies. J Hand Surg Am. 2023;48:810–821.

1.2.4. Clinical presentation

The clinical presentation of DD exhibits significant variability, determined by disease progression, healthcare accessibility, and the individual's perception of impaired quality of life. Patients often seek medical evaluation prior to the onset of contracture, which has led to the preference for the term "Dupuytren's disease" over "Dupuytren's contracture". Early diagnosis of DD proves difficult as the earliest pathologies resemble skin changes deemed normal in the aging population (42). Nonetheless, DD is primarily a clinical diagnosis, although differential diagnoses such as osteoarthritis or soft tissue neoplasms may necessitate exclusion. Skin thickening is often present with surface rippling and dimpling (**Figure 2**). Skin pits, although rare, serve as a reliable early sign of Dupuytren's disease. These pits result from deep skin retraction into the subcutaneous tissue, caused by the diseased superficial fibers of the split pretendinous band forming a dermal cord that pulls the skin inward. The apex of these cone-shaped pits is typically buried deep within the subcutaneous space and may not be visible upon macroscopic examination (43). The dorsum of the hand may present with dorsal Dupuytren's nodules, which are solid, subcutaneous masses over the dorsum of the PIP joints, or dorsal cutaneous pads, also known as knuckle pads, which involve thickening and sclerosis over the PIP or MCP joints

(44). Initial changes in the palms of patients with DD involve the formation of microcords originating from the Grapow fibers, which link the dermis to the palmar fascia. This process leads to a pseudo-callus or thickening of both the skin and the underlying subcutaneous tissue. These vertical bands are likely the first anatomical structures affected by the disease. Near the distal palmar crease, the deep subcutaneous fat undergoes fibrosis, resulting in the skin becoming tethered and adherent to the underlying fascial structures, leading to a loss of normal mobility (45). Palmar or digital nodules, adjacent to the distal palmar crease and the PIP joints, respectively, are usually painless but can be associated with stenosing tenosynovitis, which in turn can cause pain. The palmar nodules, fixed in both skin and deeper fascia, originate in the superficial components of the palmar or digital fascia. These nodules can gradually regress and precede the appearance of a cord, or cord maturation can occur without node regression. These cords, present in the palm, palmodigital area, or digits, become continuously more apparent until they resemble a tendon in consistency and appearance (9). DD demonstrates no predilection for handedness, often presenting bilaterally, albeit with asymmetric severity (46).

Figure 2. Dupuytren's disease affecting the ring finger. Source: Wikipedia, The Free Encyclopedia. Dupuytren's contracture [Internet]. San Francisco: Wikipedia, The Free Encyclopedia; 2005 [updated 2024 June 18; cited 2024 June 20]. Available from: https://en.wikipedia.org/w/index.php?title=Dupuytren%27s_contracture&oldid=1229761384

1.2.5. Diagnosis

The clinical diagnosis of typical DD is relatively straightforward. Initially, patients may notice reduced flexibility or elasticity of the palmar skin (8). Although the disease typically starts with the formation of subcutaneous nodules and palmar skin pitting, many patients present to a physician when they have already started developing cords along the path of the nodules, resulting in an inability to fully extend the affected fingers. This typical progression, although not universal, distinguishes DD from other causes of hand contracture. Additionally, knuckle pads may present on the dorsal PIPs. Generally, the distal interphalangeal joints are unaffected, but a Boutonniere deformity may develop. DD predominantly affects the ulnar side of the hand, with the ring finger being the most commonly affected (47). DD is often not only restricted to the fascia, but also the surrounding subcutaneous tissue, and the skin can be affected. Physicians should document the site of nodules, the presence of bands or cords, and angles of contractures at both the MCP and PIP joints. Additionally, any skin changes, such as pitting, dimpling or tenderness need to noted. A thorough functional history as well as the rate of progression should also be included. Disease progression is classified using a grading system: Grade 1 disease presents as a thickened nodule and a band in the palmar fascia. Grade 2 presents as a peritendinous band, and extension of the affected finger is limited. Grade 3 presents as flexion contracture (48). Staging of DD can be performed using various classification systems, including the Tubiana classification, the Meyerding classification or the Iselin classification. The Hueston tabletop test might also aid with the diagnosis. A positive result, where the patient is unable to lay their palm flat on a tabletop, may warrant further diagnostic workup for DD. While not necessary for the diagnosis, the patients should have routine bloodwork done, including HbA1C, to assess for potential risk factors. Ultrasound, computed tomography, and magnetic resonance imaging can provide a more detailed view of structures and can also be used to asses blood flow and vascular changes in the palm (49).

1.2.6. Treatment

DD remains incurable, though various treatments are available. Recurrence rates are influenced by factors such as bilaterality, age of onset below 50 years, positive family history and presence of concomitant diseases, specifically Ledderhose's, Peyronie's disease or Garrod's nodules. Higher cellularity and mitoses in resected tissue indicate a greater risk of recurrence (50). Treatment options for DD are broadly categorized into surgical or

nonsurgical options, but currently, surgical therapy is generally regarded as the most effective. Current evidence does not support the effectiveness of ultrasound therapy in treating DD (51). Electromagnetic high-energetic extracorporeal shockwave therapy is used in some instances, with some studies reporting improved post-interventional grip strength, extension range and patient-reported outcomes (52, 53). Cross-frictional massage and stretching offer temporary improvement in range of motion, but effects regress within three months without morphological changes detectable by ultrasound. Temperature-controlled high-energy laser therapy is associated with decreased pain and improved patient-reported outcomes over a three-month follow-up period, though it does not alter the extension deficit (54). Historical use of human enzyme injections such as pepsin, trypsin, hyaluronidase, and thiosinamin throughout the 20th century was largely unsuccessful (55). Local injections of corticosteroid depots are widely used in painful nodules without contractures, though their efficacy remains debated (56). Clostridial collagenase, another type of injection, that dissolves type I and III collagen, presents challenges due to its lack of tissue specificity and is linked to higher recurrence rates and lower deformity correction compared to open fasciectomy (57). Radiotherapy is commonly employed in early-stage DD in centers with therapeutic experience. Radiotherapy is highly effective for patients with extension deficits of less than 10 degrees and without contractures; however, its efficacy significantly diminishes as the degree of extension deficits increases (58). The dose-dependent risk of adverse effects, including malignancy in younger patients, must be considered.

Surgical options for treating DD are numerous. Limited fasciectomy is the most common surgical approach in many countries (**Figure 3**). In this procedure, only pathological tissue is excised, while unaffected structures are preserved. This approach is typically taken when nodules are painful and do not respond to conservative measures or in cases of progressing contractures of angles between 30 and 60 degrees. Complications may include damage to the neurovascular bundles, as those are displaced and shortened, or delayed wound healing (59). Another disadvantage is that it takes patients around 6 weeks to be able to use the hand again. Recurrence rates are reported between 2% and 73% (60), but even repeated limited fasciectomy is safe, effective and connected to high levels of patient satisfaction (61). Segmental fasciectomy, which involves removing short, 1-cm segments of the diseased fascia, offers similar recurrence rates but quicker patient recovery (62). Radical fasciectomy, in which the fascia is widely removed, but the overlying skin is

preserved (63). Due to a high incidence of complications, radical fasciectomy is rarely performed anymore. The open palm technique, where the skin over the TLPF is left open to allow for wound drainage, results in fewer peri- and postoperative complications but an extended wound healing duration (64). Dermatofasciectomy describes the approach in which the affected fascia is excised together with the overlying skin. A skin graft is then used to cover the produced defect. This approach is primarily used in patients with very high risk of recurrence or recurrent skin involvement. While this process reduces recurrence risk, the disadvantages of fasciectomy prevail, with the added disadvantages of harvesting and applying the skin graft (65). Percutaneous needle fasciectomy (PNF), being minimally invasive, is now widely popular for treating DD with contractures less than 90 degrees (66). PNF involves cutting the affected cords under local anesthesia with an injection needle. Recurrence rates are significantly higher than after limited fasciectomy, and in some cases, limited fasciectomy might eventually still be unavoidable. Despite these higher recurrence rates, PNF offers lower cumulative complications and faster recovery, making it suitable for elderly patients or those accepting the possibility of earlier recurrence. For younger patients with high recurrence risk, limited fasciectomy remains preferable (67). While pre- and postoperative splinting have not demonstrated functional benefits, they lead to increased follow-up of patients which is of high importance. Splinting may also be considered in a special subset of patients who are deteriorating after their initial postoperative review (68).

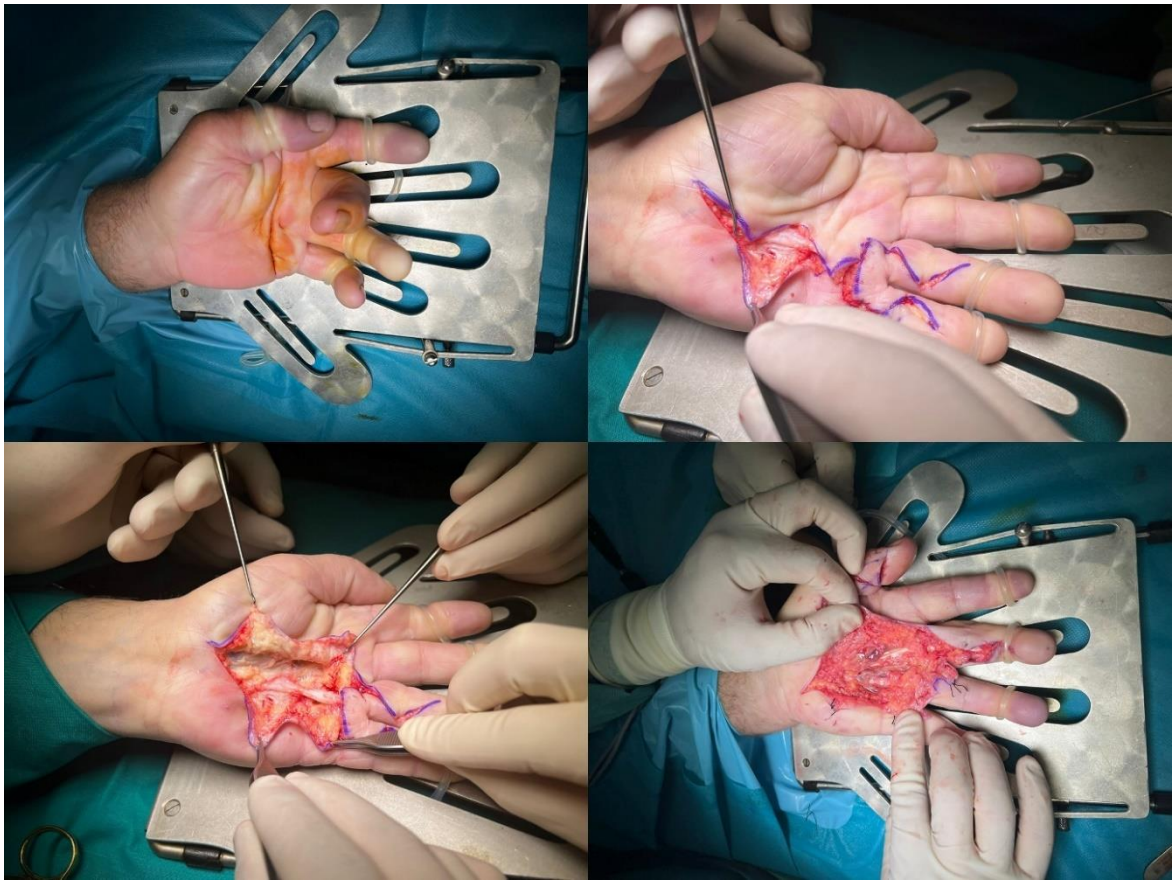

Figure 3. Fasciectomy of a patient with Dupuytren's disease. Source: Images were provided by courtesy of Ivo Tripković, MD, PhD, from his personal archive.

1.3. Epithelial–to-mesenchymal transition

Epithelial–to-mesenchymal transition (EMT) is a biological process where epithelial cells undergo a phenotypic and biochemical shift to a mesenchymal state, characterized by reduced intercellular adhesion, loss of polarity, increased motility, invasiveness, resistance to apoptosis, and enhanced ECM production (69). The induction of EMT is mediated by signaling molecules that activate distinct signaling pathways, which in turn stimulate a set of transcription factors (TFs) that regulate EMT. These master regulators include SNAIL family proteins (SNAI1 and SNAI2), zinc finger E-box binding homeobox proteins (ZEB1 and ZEB2), and TWIST family proteins (TWIST1 and TWIST2). Collectively, these TFs suppress the expression of epithelial markers such as E-cadherin, mucin-1, PTEN, and RKIP, while activating mesenchymal markers such as N-cadherin, vimentin, vitronectin, and matrix metalloproteinases. Additionally, EMT TFs also modulate the expression of tight junction proteins such as claudins and occludins, as well as gap junction components. The reduced expression of these junctional proteins leads to decreased cell-cell attachment, facilitating the EMT process (70).

1.3.1. EMT subtypes

There are three major types of EMT, each occurring in one of three distinct biological contexts and each with distinct consequences (**Figure 4**). Type 1 EMT is integral to implantation, embryogenesis, and organ development. This type generates different cell types sharing a common mesenchymal phenotype. Unlike type 2 and type 3 EMT, it does not induce fibrosis or systemic dissemination via circulation. Type 2 EMT occurs in wound healing, tissue regeneration, and organ fibrosis. Initiated as part of healing processes, it generates fibroblasts for tissue repair. Unlike type 1, type 2 EMT is linked to inflammation and ceases after the inflammation subsides. However, in organ fibrosis, continuous inflammation leads to persistent tissue destruction, leading to continuous type 2 EMT activation. Type 3 EMT occurs in neoplastic cells with genetic and epigenetic changes, promoting clonal growth and localized neoplasm development. This form of EMT endows cancer cells with invasive and metastatic capabilities, contributing to life-threatening cancer progression (71).

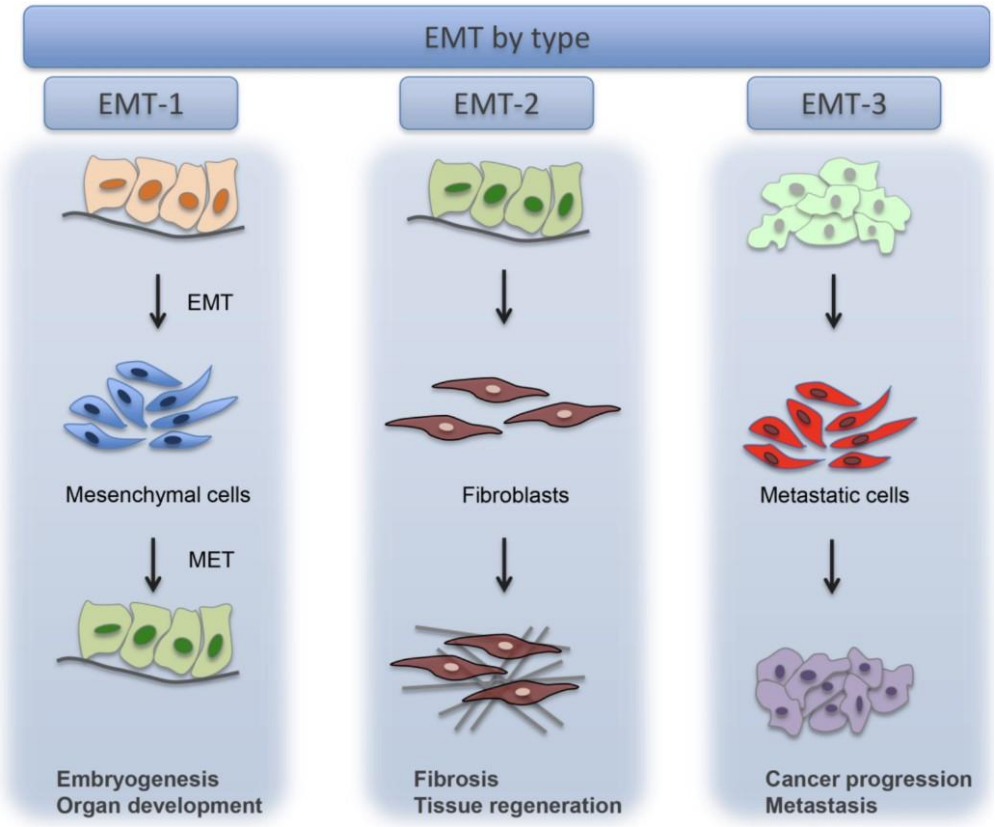

Figure 4. Main subtypes of EMT. Source: Marconi GD, Fonticoli L, Rajan TS, Pierdomenico SD, Trubiani O, Pizzicannella J, et al. Epithelial-mesenchymal transition (EMT): the type-2 EMT in wound healing, tissue regeneration and organ fibrosis. Cells. 2021;10:1587.

Multiple rounds of type 1 EMT and its reverse process, mesenchymal-to-epithelial transition (MET) are observed during the three-dimensional organogenesis of the embryo (72). According to the spatial development, type 1 EMT is further subdivided into primary, secondary and tertiary. Primary EMT occurs during implantation, gastrulation and neural crest formation. EMT is fundamental during gastrulation, enabling cells to separate from the epiblast layer and migrate to specific regions within the embryo, such as the primitive streak, to form the three germ layers. Post-gastrulation, the cuboidal epithelium in the ectoderm forms the neural plate and its lateral border becomes the neural crest. Neural crest cells undergo EMT, which allows them to migrate to their target sites, differentiating into most components of the peripheral nervous system (neurons and glial cells), melanocytes, endocrine cells, and craniofacial structures (73). These primary EMT events are followed by differentiation events, during which these cells undergo MET and transiently form epithelial structures such as the notochord, somites, urogenital precursors, somatopleure, and splanchnopleure. Except for the notochord, these secondary epithelia experience a secondary EMT, producing mesenchymal cells with more restricted differentiation potential. Tertiary EMT occurs during the formation of cushion mesenchyme from the atrioventricular canal or the outflow tract of the heart (74). Type 1 EMT can be activated by various signaling molecules. For instance, EMT during gastrulation is triggered by the canonical WNT signaling pathway, TGF-β superfamily proteins, and growth factors.

Type 2 EMT is observed in response to inflammation, during wound healing and tissue regeneration and is terminated once repair is completed. During wound healing, keratinocytes at the wound edge undergo partial EMT, acquiring a metastable state that allows movement while maintaining loose contact with their surroundings. These cells then differentiate into fibroblast-like cells to rebuild tissues following trauma or inflammatory damage. Additionally, type 2 EMT gives origin to myofibroblasts from epithelia in reparative fibrosis. If the inflammation is chronic, the elevated formation of myofibroblasts leads to progressive fibrosis due to excessive ECM deposition and parenchymal destruction (75). Type II EMT can be induced by vascular endothelial growth factor (VEGF) and TGF-β.

The third subtype of EMT occurs in epithelial cancer cells and is associated with changes in oncogenes and tumor suppressor genes. Cells undergoing type 3 EMT can invade tissues and metastasize through the bloodstream, leading to systemic cancer progression. While the signaling pathways for type 1 and 2 EMT are well understood, the

specific signals inducing type 3 EMT in epithelial carcinoma cells are still not fully elucidated (71). Neoplastic cells often show incomplete conversion, expressing both epithelial and mesenchymal markers. This partial EMT induces stem cell-like properties in those cells, leading to advantages in survival and sustenance in the host (69). Type 3 EMT is known to be induced by a large set of signaling molecules (WNT, TGF-β, VEGF, etc.) with new inducers being continuously discovered.

1.3.2. EMT in Fibrosis

During tissue repair, myofibroblasts play a crucial role depositing ECM and rebuilding the damaged parenchymal tissue architecture. However, when the production of ECM continues and exceeds its degradation, this reparative process becomes progressive fibrosis, leading to tissue architecture disruption and organ dysfunction (**Figure 5**). As mentioned previously, type 2 EMT is closely related to fibrogenesis. TGF-β is a well-known inducer of EMT, and its production can be caused by inflammation, hypoxia and senescence. In inflammation, helper T-cells produce IL-17 which induces inflammatory cell infiltration. These cells in turn generate pro-inflammatory cytokines (tumor necrosis factors, IL-6, IL-1) which stimulate further inflammatory cell infiltration. This inflammatory cascade stimulates EMT and if persistent, causes excessive ECM accumulation (76). Under hypoxic conditions, inactivation of prolyl hydroxylases leads to accumulation and activation of hypoxia-inducible factor-alpha which induces EMT-related gene expression of SNAIL1, TWIST1 and BMI1. These TFs suppress epithelial marker expression and induce the expression of mesenchymal markers, leading to EMT and progressive fibrosis (77). In senescence, cells enter cell-cycle arrest. They remain metabolically active, entering the senescence-associated secretory phenotype. In this state, they secrete cytokines that attract leukocytes, causing the leukocytes to secrete pro-inflammatory cytokines, sustaining an inflammatory environment conducive to EMT (78). Senescence might also be triggered by p53-mediated reactive oxygen species production (79). Increased markers of senescence as well as mesenchymal markers were found in multiple organ fibrosis (80). The exact pathways are variable and have only been shown in few specific organs and mice.

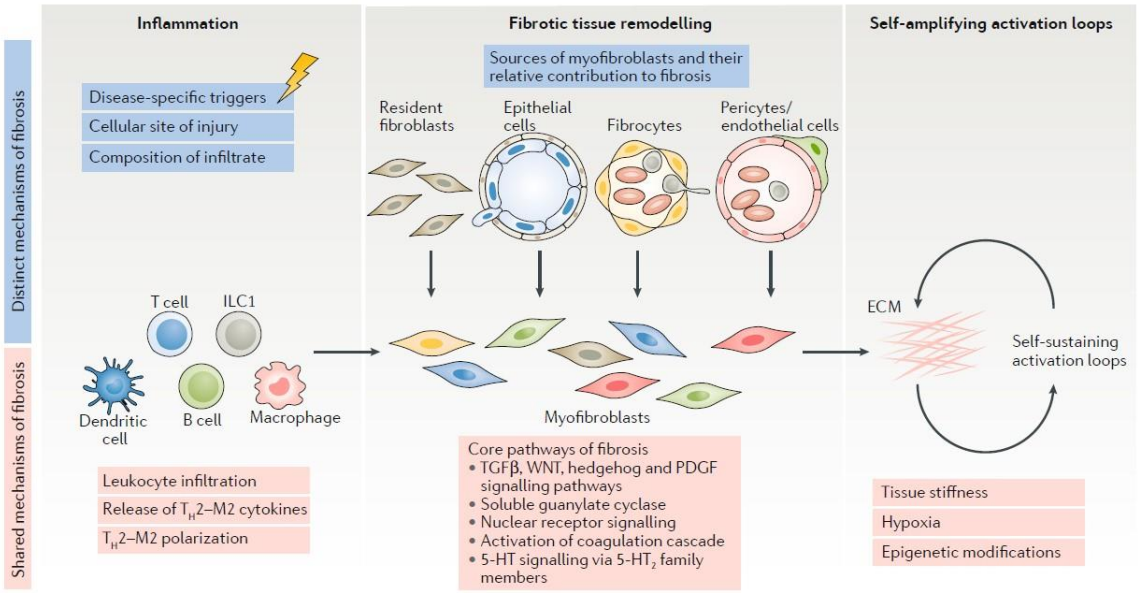

Figure 5. General mechanisms of fibrosis. Source: Distler JHW, Györfi A-H, Ramanujam M, Whitfield ML, Königshoff M, Lafyatis R. Shared and distinct mechanisms of fibrosis. Nat Rev Rheumatol. 2019;15:705-30.

In organ-specific fibrosis, only certain cells specific to that organ undergo EMT. In the lung, bronchial and alveolar epithelial cells can lead to peribronchial and alveolar septal fibrosis, respectively (81, 82). Additionally, pleural mesothelial cells exhibit mesothelial-to-mesenchymal transformation, another type of EMT, in the pathogenesis of idiopathic pulmonary fibrosis (83). In the liver, hepatic stellate cells are considered the primary source of myofibroblasts after liver parenchymal destruction (84). The role of hepatocytes and cholangiocytes in liver fibrosis and EMT remains controversial. Tubular epithelial cells are the primary cells undergoing EMT in the kidney (85). Emerging evidence however indicates that those cells undergo partial EMT, expressing both epithelial and mesenchymal markers (86). This partial EMT is believed to contribute to fibrosis by loss of epithelial regeneration rather than by fibroblast generation (87). Aside from the tubular epithelial cells, podocytes and endothelial cells also contribute to renal fibrosis (88). In inflammatory bowel disease patients, chronic and recurrent intestinal inflammation leads to progressive fibrosis. In Crohn's disease specifically, fistula formation is also tied to EMT of the intestinal epithelium (89). Patients undergoing peritoneal dialysis may develop peritoneal fibrosis due to dialysate exposure. Mesothelial-to-mesenchymal transformation, which is seen in early peritoneal fibrosis, indicates mesothelial involvement (90). Post-myocardial infarction and in conditions like valve dysfunction and atherosclerosis, cardiac tissue healing involves EMT (91). The epicardial cells stimulated by WNT1 in animal models as

well as by injury in vivo, showed EMT, initiating tissue repair and angiogenesis (91, 92). EMT is fundamental in fibrotic cataract pathogenesis, both under hyperglycemic conditions and post-cataract surgery (93). While other organs have various cells with the potential to give origin to myofibroblasts, in the lens there are no resident fibroblasts, so all myofibroblasts have to be derived from the epithelial cells of the lens (94). EMT is also observed in cutaneous fibrotic diseases, such as scleroderma and keloids. In scleroderma, myoepithelium of the eccrine sweat glands undergoes EMT, increasing concentrations of αSMA, fibronectin and TGF-β1, while reducing E-Cadherin (95). Keloid formation involves EMT of keratinocytes, evidenced by vimentin positivity and spindle-shaped morphology typical of myofibroblasts (96).

1.3.3. Endothelial-to-mesenchymal transition

Endothelial-to-mesenchymal transition (EndoMT) describes a process in which, similar to EMT for epithelial cells, loss of inherent endothelial markers and acquisition of mesenchymal markers occur (**Figure 6**). Functionally, these cells lose tight junctions, increase secretion of ECM proteins, gain increased motility and enhanced resistance to apoptosis (97). EndoMT, first described in cardiac embryogenesis, involves key molecular pathways, notably TGF-β and bone morphogenetic proteins (BMPs) (98). The interaction of the TGF-β/BMP ligands with serine/threonine kinase receptors on endothelial cells initiates intracellular signaling cascades, leading to the activation of TFs such as SNAI1, SNAI2, TWIST1, ZEB1, and ZEB2. These TFs downregulate endothelial markers and upregulate mesenchymal markers, facilitating EndoMT (99). In addition to TGF-β/BMP pathways, WNT/β-catenin and NOTCH signaling pathways, known from EMT, are involved in EndoMT. These pathways can synergize and modulate each other, enhancing the transition process (100). Notably, fibroblast growth factor (FGF) and hepatocyte growth factor have been demonstrated to inhibit EndoMT by antagonizing the effects of TGF-β1 (101). Knockout studies of FGF receptor 1 (FGFR1) reveal that its absence activates TGF-β1-induced EndoMT, which subsequently contributes to intimal hyperplasia and stenosis, commonly observed in various cardiovascular diseases (102). Additionally, endothelial cells possess the capability to secrete FGF2, which functions to counteract TGF-β-induced EndoMT. This inhibitory role of FGFs may be mediated by specific anti-EndoMT microRNAs (103). Furthermore, endothelin-1 promotes EndoMT via the TGF-β pathway. Inhibition of endothelin-1 has been suggested as a therapeutic approach to mitigate diabetic-induced cardiac fibrosis (104).

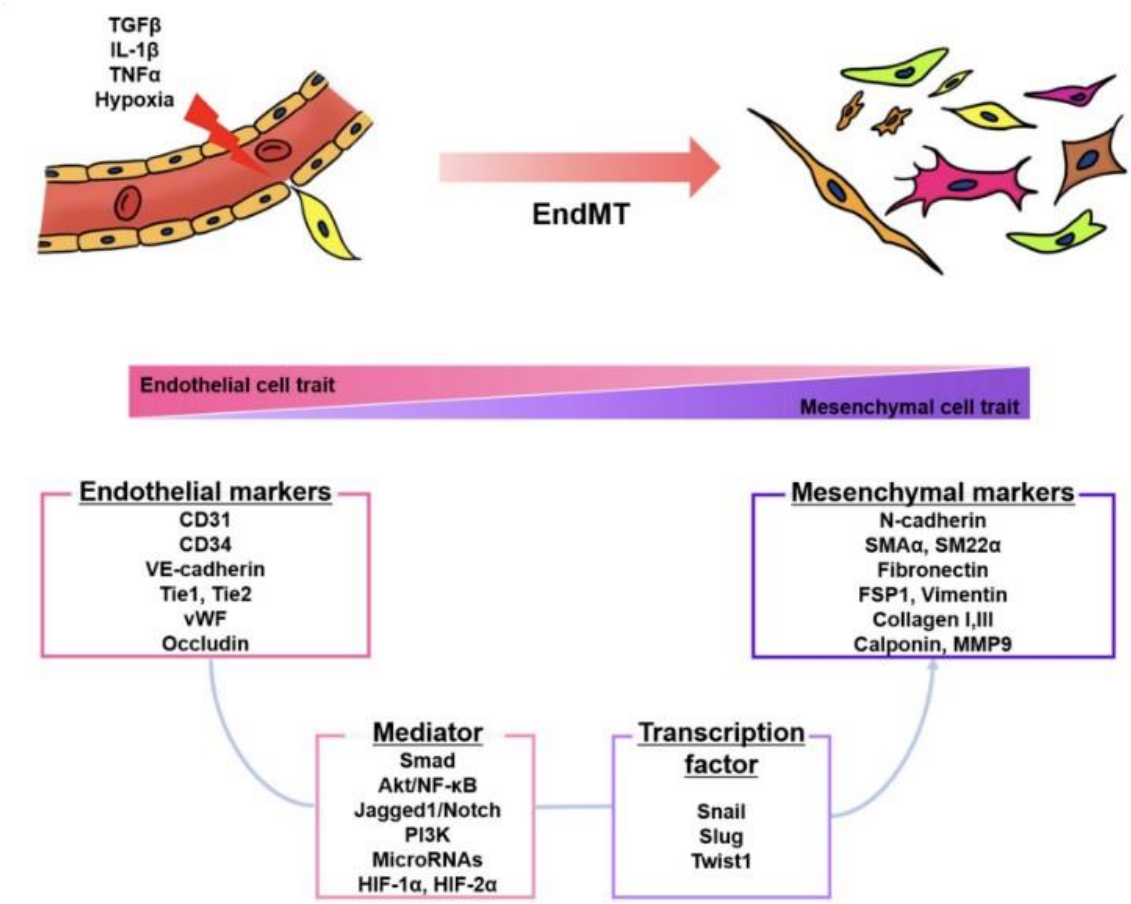

Figure 6. Schematic representation of the EndoMT process. Source: Yun E, Kook Y, Yoo KH, Kim KI, Lee M-S, Kim J, et al. Endothelial to mesenchymal transition in pulmonary vascular diseases. Biomedicines. 2020;8:639.

The degree in which EndoMT contributes to fibrosis remains a topic of ongoing debate. However, recent investigations have identified EndoMT as a potential additional source of fibroblasts in fibrotic organs (105). The origin and composition of fibroblasts in organ-specific fibrosis exhibit significant variability. In the context of systemic sclerosis, there is compelling evidence for the existence of endothelial cells co-expressing both endothelial and mesenchymal markers and exhibiting a distinct contractile, spindle-shaped phenotype (106, 107). EndoMT in the walls of capillary vessels can lead to an increase in perivascular profibrotic myofibroblasts, coupled with a concurrent loss of endothelial cells. This phenomenon establishes a unique connection between tissue fibrosis and destructive vasculopathy. Clinically, this manifests as capillary rarefaction and impaired angiogenesis in systemic sclerosis skin (108). When affecting arterioles and small arteries, EndoMT may play a role in the development of fibroproliferative vasculopathy. This condition is characterized by the accumulation of myofibroblasts within the vessel subintima and

media, leading to vessel wall thickening and occlusive vascular disease (107). EndoMT has also been shown to contribute to fibrosis in the lungs, kidneys and liver (109). The dual role of EndoMT in promoting both vascular pathology and tissue fibrosis highlights its potential as a future research objective and therapeutic target in the management of systemic sclerosis and other fibrotic diseases (110).

2. OBJECTIVES

Aim:

The aim of this study was to analyze the expression of endothelial and mesenchymal markers, as well as an EndoMT-related TF, in the palmar fascia of patients with DD and in healthy palmar fascia in order to determine whether EndoMT is associated with the fibrosis in DD.

Hypotheses:

1. The expression of endothelial markers will be decreased in the endothelial cells of the palmar fascia of DD patients compared to healthy palmar fascia tissue.

2. The expression of mesenchymal markers will be increased in the endothelial cells of the palmar fascia of DD patients compared to healthy palmar fascia tissue.

3. The expression of the EndoMT-related TF will be present in the endothelial cells of the palmar fascia of DD patients.

3. MATERIALS AND METHODS

3.1. Sample collection and initial processing

Palmar fascia samples were originally collected during routine surgical procedures at the Department of Plastic Surgery of the University Hospital in Split between March 2021 and March 2022. Informed consent was obtained from all patients for the use of their tissues. The procedures were approved by the Ethical and Drug Committee of the University Hospital in Split (class: 500-03/21-01/36, registry number: 2181-147-01/06/M.S.-20-02) and adhered to the Declaration of Helsinki and other relevant national guidelines and regulations. All samples underwent the same initial processing steps. After fixation in a 4% paraformaldehyde solution in phosphate-buffered saline (PBS) and dehydration in ethanol solutions with increasing concentrations (from 70% to 100% ethanol), the samples were cleared using xylene solutions, infiltrated with melted paraffin in an oven and embedded by cooling to room temperature. Excess paraffin was trimmed before cutting the samples into 5 μm-thick serial sections using a microtome and mounting them on glass slides. The samples were then archived at the Department of Histology and Embryology of the University of Split School of Medicine for use in future studies. The Ethics committee from the University of Split School of Medicine approved the use of these archived samples for the purpose of this thesis (class: 029-01/24-02/0001, registry number: 2181-198-03-04-24-0041). Samples from 5 patients with carpal tunnel syndrome and 5 patients with DD were taken and categorized into three groups: palmar fascia from patients with carpal tunnel syndrome (control samples, CTRL), fibrotic cords from patients with DD (DDFC), and macroscopically unaffected palmar fascia next to the fibrotic cords from patients with DD (DDUF).

3.2. Hematoxylin and eosin staining

The tissue sections were deparaffinized using xylene and rehydrated with graded ethanol solutions to prepare them for hematoxylin and eosin staining. After being immersed for 10 minutes in a hematoxylin solution, the samples were washed in distilled water. Subsequently, the sections were covered with an eosin solution for 10 minutes and once again rinsed with distilled water. Dehydration with ethanol solutions and treatment with xylene solutions were performed to prepare the samples for coverslipping with Canada balsam. The sections stained with hematoxylin and eosin were analyzed using an Olympus BX51 microscope (Olympus, Tokyo, Japan) and

images were captured using a Nikon DS-Ri2 mounted digital camera (Nikon, Tokyo, Japan) and NIS-Elements F software (Nikon, Tokyo, Japan).

3.3. Immunofluorescence staining

After deparaffinization and rehydration of the sample sections, antigen retrieval (release of epitopes) was performed by submerging the sections in a 0.01 M sodium citrate buffer solution (pH 6.0) and heating them in a steam cooker for 30 minutes at 95°C. The sections were cooled to room temperature and rinsed in a 0.1 M PBS solution for 5 minutes. The sections were then treated with a protein blocking buffer (Protein Block, Abcam, Cambridge, United Kingdom) for 20 minutes in a humid chamber to prevent nonspecific binding of antibodies to the tissue samples. The sections were incubated with combinations of primary antibodies diluted in PBS (**Table 1**) in a humid chamber overnight, after which they were washed twice in PBS solutions. Antibodies against the endothelial markers von Willebrand factor (vWF) and cluster of differentiation 31 (CD31), mesenchymal markers vimentin and αSMA, and the EndoMT-related TF SNAI2 were used. This was followed by an application of appropriate secondary antibodies (**Table 1**) and incubation in a humid chamber for one hour before an additional three rounds of washing in PBS solutions, each lasting 5 minutes. A 4',6-diamidino-2-phenylindole (DAPI) solution was used to cover the sections for 2 minutes to counterstain nuclei. After rinsing off the DAPI solution with distilled water, the sections were coverslipped using the Immumount mounting medium (Thermo Shandon, Pittsburgh, USA). The specificity of the staining was controlled by the omission of primary antibodies from the protocol, which resulted in the absence of any specific staining. The sections were examined and images were captured using the same microscope, camera, and software as for the sections stained with hematoxylin and eosin.

Table 1. Primary and secondary antibodies used in the study.

	Antibody	Host	Dilution	Catalog number	Source
Primary	CD31 (PECAM-1) (89C2)	Mouse	1:400	3528	Cell Signaling Technology, Danvers, USA
	VWF (D8L8G)	Rabbit	1:400	65707	Cell Signaling Technology, Danvers, USA
	Vimentin (D21H3)	Rabbit	1:400	5741	Cell Signaling Technology, Danvers, USA
	αSMA	Mouse	1:400	M0851	DAKO, Glostrup, Denmark
	Slug (SNAI2) (C19G7)	Rabbit	1:200	9585	Cell Signaling Technology, Danvers, USA
Secondary	Anti-Mouse IgG, Alexa Fluor® 488	Donkey	1:300	715-545-150	Jackson Immuno Research Laboratories, Inc., Baltimore, USA
	Anti-Rabbit IgG, Alexa Fluor® 488	Donkey	1:300	711-545-152	Jackson Immuno Research Laboratories, Inc., Baltimore, USA
	Anti-Mouse IgG, Rhodamine Red™-X	Donkey	1:300	715-295-151	Jackson Immuno Research Laboratories, Inc., Baltimore, USA
	Anti-Rabbit IgG, Rhodamine Red™-X	Donkey	1:300	711-295-152	Jackson Immuno Research Laboratories, Inc., Baltimore, USA

3.4. Fluorescent signal quantification

The immunofluorescence signal associated with the analyzed proteins was quantified by calculating the area percentage taken up by the signal in the captured images. For each sample, we captured ten nonadjacent representative images at x400 total magnification, resulting in a total of 50 images for analysis per sample group and per analyzed protein. Each image underwent identical processing steps. Images taken for analysis were uploaded to the free online image editor Photopea ([internet], https://www.photopea.com/). In the editor, blood vessels found in the captured images were selected with the “Lasso” tool and cut out from the original images and placed

into blank images that had identical dimensions. Those images were then saved in the form of Tagged Image File Formats and opened using ImageJ software (NIH, Bethesda, USA). To purify the fluorescent signal of the analyzed protein, we have subtracted the red color channel from proteins marked with green fluorescence (vWF and CD31) and the blue color channel from the protein marked with red fluorescence (vimentin). The resulting images were duplicated and filtered using the median filter with a radius of 5 for vWF and CD31, while a radius of 20 was used for vimentin. The definitive positive signal was then isolated by subtracting the filtered images from the unfiltered images. The final images were transformed into 8-bit images and the "Triangle" method was used for thresholding. The "Analyze particles" function was used to determine the area percentage that the isolated fluorescent signal takes up in the entire image. Since parts of the analyzed images had no tissue, they were completely devoid of any fluorescent signal which resulted in the measured area percentage being lower than it actually would have been had the tissue been present throughout the captured images. A correction of the area percentage measurement was made by calculating the number of total pixels of the images and the number of pixels found in the empty spaces by using the "Magic Wand" tool in Photopea. The definitive area percentage was calculated by multiplying the originally measured area percentage with the number of total pixels and dividing it by the difference between total and empty space pixels. This value was used for all statistical analyses. Figures were assembled using Adobe Photoshop version 21.0.2 (Adobe, San Jose, USA).

3.5. Statistical analysis

Statistical analyses were conducted using GraphPad Prism version 9.0.0 software (GraphPad Software, San Diego, USA). All results are expressed as the mean and standard deviation of the area percentages of the analyzed proteins. The normality of the data distribution was assessed with the Kolmogorov–Smirnov test. A two-way analysis of variance (ANOVA) with Tukey's post hoc test was employed to determine whether statistically significant differences in protein expression between the analyzed sample groups exist. A *P*-value of less than 0.05 was considered statistically significant.

4. RESULTS

The preservation of normal tissue morphology of the analyzed samples was confirmed by hematoxylin and eosin staining (**Figure 7**). The blood vessels in CTRL samples were found in the areas of loose connective tissue, while the majority of the samples consisted of dense connective tissue. A similar finding was present in DDUF samples, with blood vessels being present in areas of loose connective tissue between bands of dense connective tissue. The DDFC samples predominantly contained highly cellular dense connective tissue in the form of bands and nodes, while blood vessels were confined to the narrow strips of loose connective tissue around them.

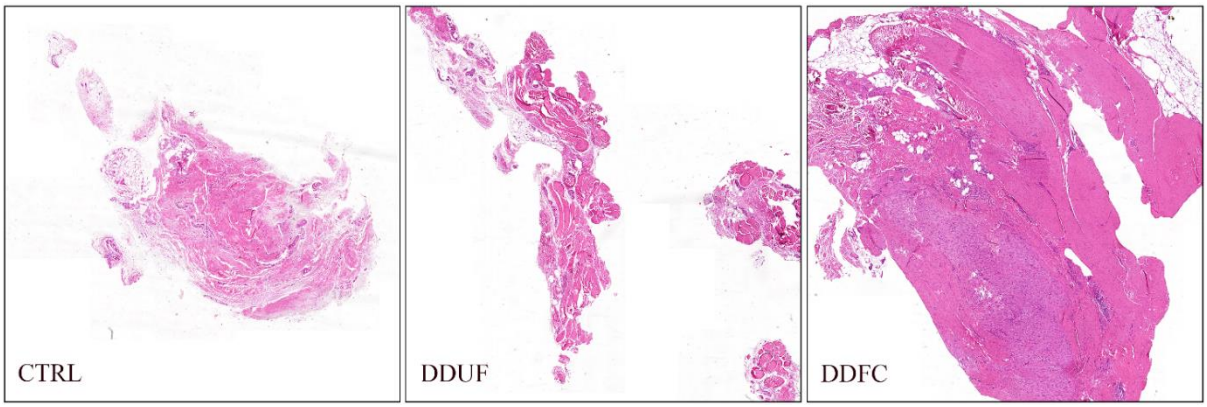

Figure 7. Hematoxylin and eosin staining of the analyzed samples. CTRL – palmar fascia of patients with carpal tunnel syndrome, DDUF - macroscopically unaffected palmar fascia from patients with Dupuytren's disease (DD), DDFC – fibrotic cords from patients with DD.

The first combination of proteins that was analyzed consisted of vWF, an endothelial marker, and αSMA, a mesenchymal marker (**Figure 8**). In the CTRL samples, vWF demonstrated a granular cytoplasmic staining pattern of high intensity in endothelial cells and no positivity in any other cells. αSMA showed strong positivity in pericytes and the smooth muscle cells of the vascular walls, while endothelial cells were negative for αSMA staining. The expression of vWF in the endothelial cells of DDUF samples was visibly reduced compared to CTRL samples, both in the amount and intensity of the signal. The same was true for DDFC samples, with vWF expression becoming even more sparse compared to CTRL samples. The vWF signal was confined to endothelial cells in both DDUF and DDFC samples. There were no significant differences visible between the sample groups regarding αSMA staining and no endothelial cells displayed αSMA positivity.

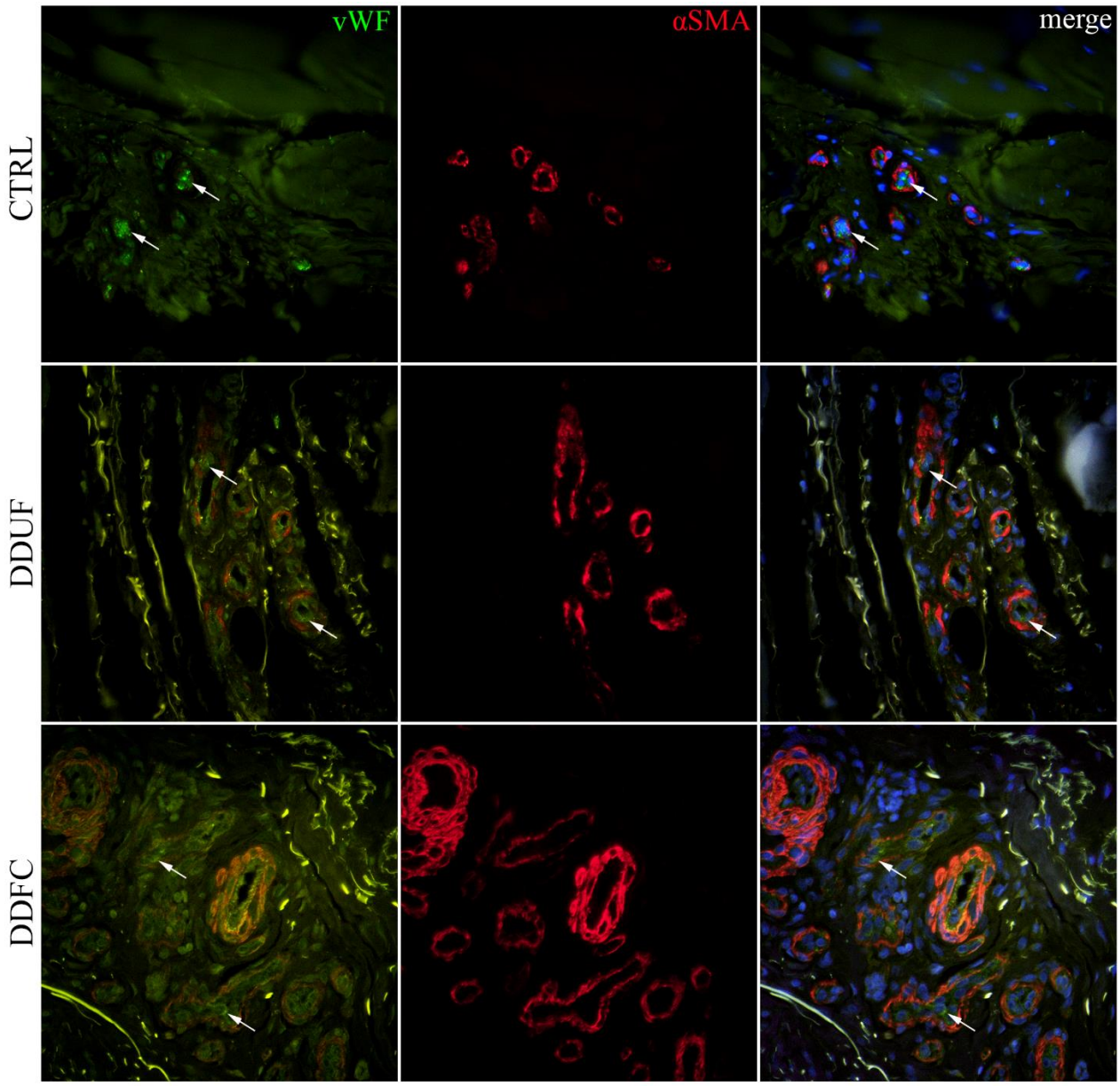

Figure 8. Expression of von Willebrand factor (vWF) and alpha-smooth muscle actin (αSMA) in the analyzed samples. CTRL – palmar fascia of patients with carpal tunnel syndrome, DDUF - macroscopically unaffected palmar fascia from patients with Dupuytren's disease (DD), DDFC – fibrotic cords from patients with DD. The first panels (green signal) represent the staining for vWF, while the second panels (red signal) represent αSMA staining. The third panels represent the first two panels merged together with the nuclear staining (blue signal). Arrows mark endothelial cells positive for vWF. All images were taken at x400 total magnification.

The second combination that was analyzed contained the endothelial marker CD31 and the mesenchymal marker vimentin (**Figure 9**). The CTRL samples revealed the normal distribution of the analyzed proteins. CD31 showed a strong membranous staining pattern in endothelial cells, while no other cells displayed any CD31 positivity. Vimentin on the other hand demonstrated a fibrillar cytoplasmic staining pattern of moderate intensity in the endothelial cells, smooth muscle cells and surrounding fibroblasts. When compared to CTRL samples, a marked reduction in the amount of CD31 staining was visible in DDUF samples, while DDFC samples showed an even greater depletion of the CD31 signal. The expression of vimentin became stronger in some endothelial cells of DDUF samples and many endothelial cells of DDFC samples compared to the CTRL samples. While CD31 was exclusively found in the endothelial cells of CTRL and DDUF samples, a cell positive for both CD31 and vimentin was found in the connective tissue surrounding the blood vessels of a DDFC sample, likely representing a cell undergoing the EndoMT process (**Figure 10**).

Statistical analysis of the expression of the analyzed proteins, measured by the area percentage taken up by their associated fluorescent signal, revealed significant differences between the sample groups (**Figure 11**). The expression of vWF was significantly higher in the endothelial cells of CTRL samples (1.97% ± 0.94%) compared to both DDUF (1.09% ± 0.30%; $P < 0.001$) and DDFC samples (0.62% ± 0.23%; $P < 0.001$). The expression in DDFC samples was significantly lower ($P = 0.012$) than in DDUF samples. αSMA was not expressed in endothelial cells in any of the samples, so no formal analysis was performed. The area percentage of the CD31 signal was also significantly higher in the endothelial cells of CTRL samples (2.12% ± 1.80%) compared to DDUF (1.21% ± 0.35%; $P < 0.001$) and DDFC samples (0.59% ± 0.18%; $P < 0.001$). Once again, the expression in DDFC samples was significantly lower ($P = 0.016$) than in DDUF samples. The analysis of vimentin expression revealed that DDFC samples (28.29% ± 5.02%) had a significantly higher area percentage in endothelial cells compared to CTRL (24.26% ± 5.89%; $P = 0.003$) and DDUF samples (25.17% ± 4.88%; $P = 0.030$).

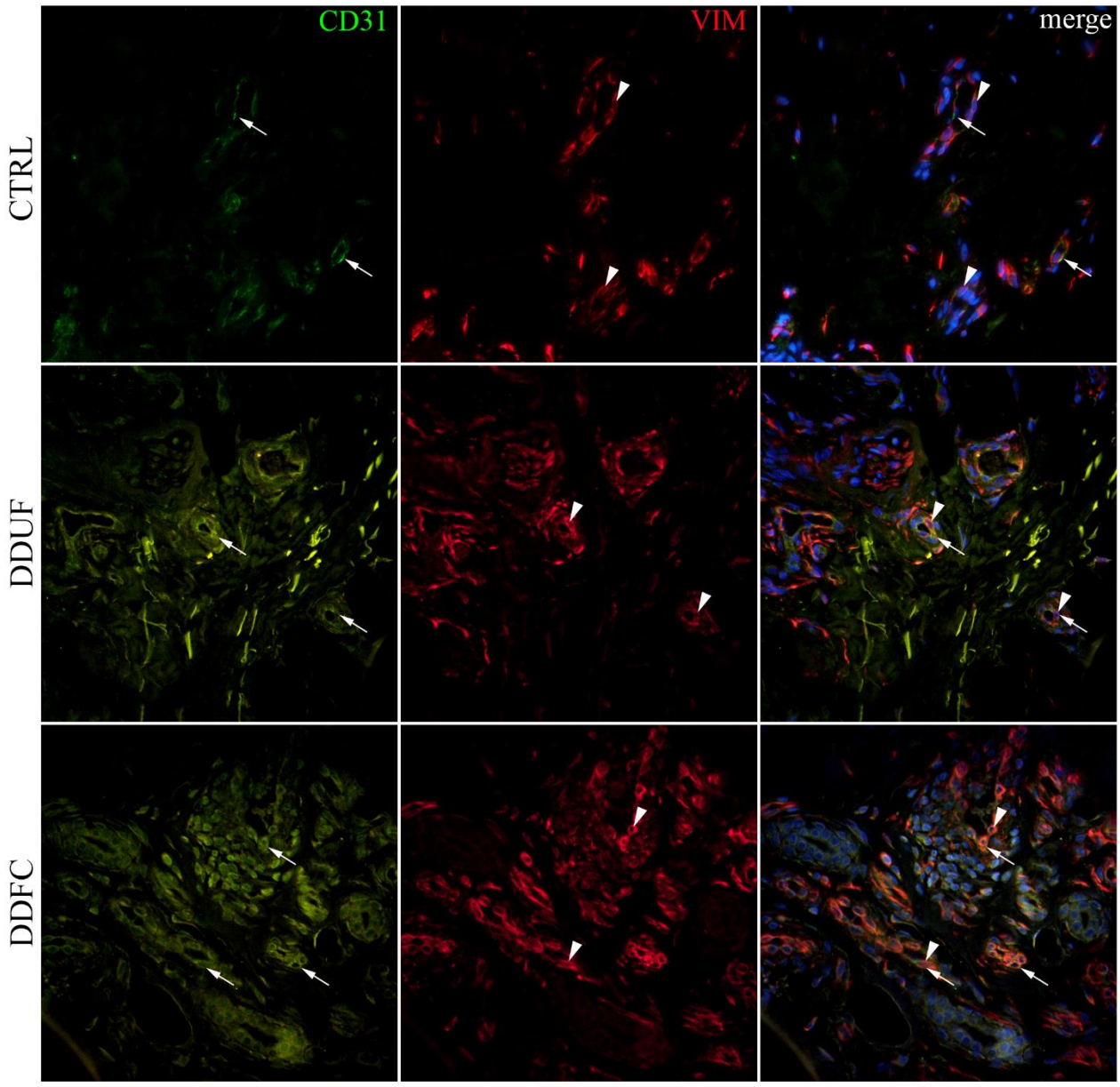

Figure 9. Expression of cluster of differentiation 31 (CD31) and vimentin (VIM) in the analyzed samples. CTRL – palmar fascia of patients with carpal tunnel syndrome, DDUF - macroscopically unaffected palmar fascia from patients with Dupuytren's disease (DD), DDFC – fibrotic cords from patients with DD. The first panels (green signal) represent the staining for CD31, while the second panels (red signal) represent VIM staining. The third panels represent the first two panels merged together with the nuclear staining (blue signal). Arrows mark endothelial cells positive for CD31 and arrowheads mark cells positive for VIM. All images were taken at x400 total magnification.

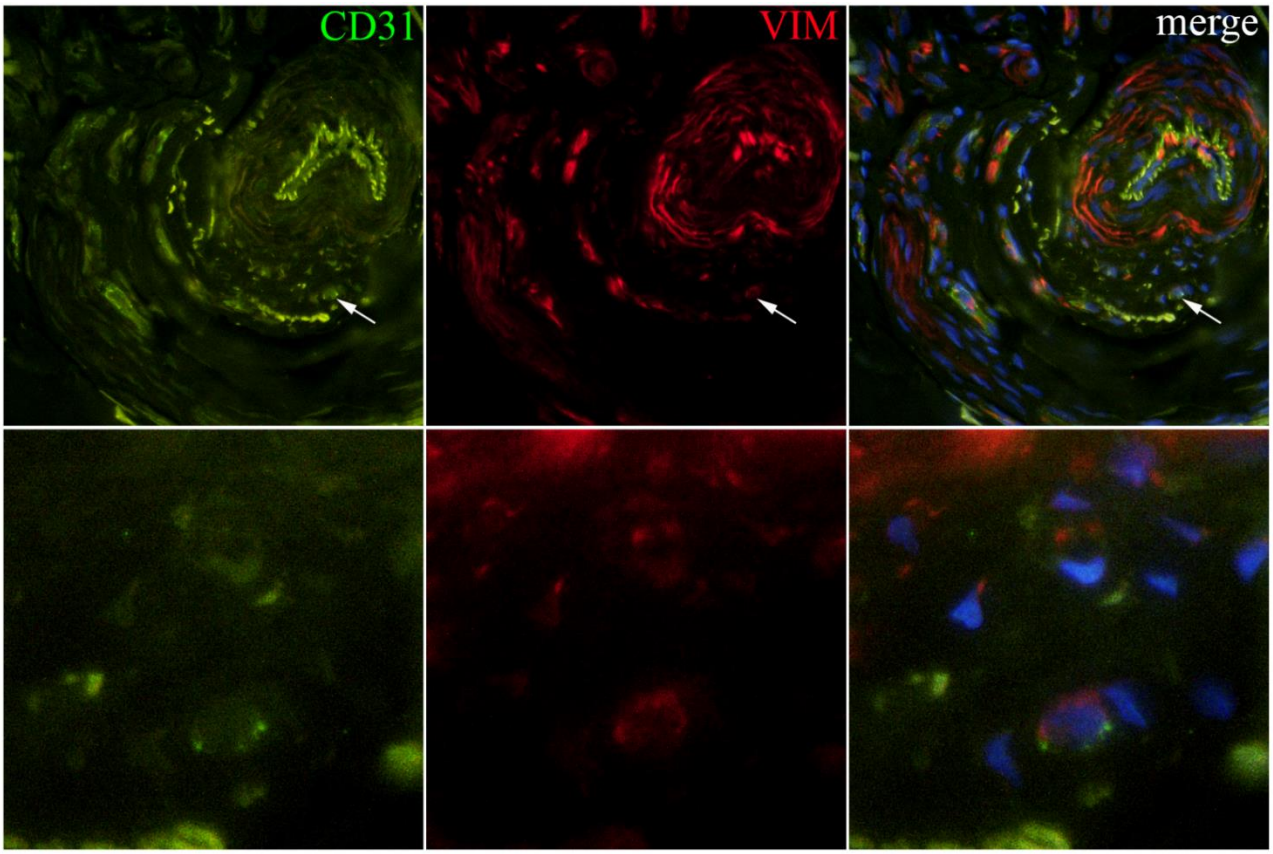

Figure 10. A cell undergoing endothelial-to-mesenchymal transition in a fibrotic cord sample of a patient with Dupuytren's diesease. The first panels (green signal) represent the staining for cluster of differentiation 31 (CD31), while the second panels (red signal) represent vimentin (VIM) staining. The third panels represent the first two panels merged together with the nuclear staining (blue signal). The arrows mark the CD31+ VIM+ cell outside blood vessels. The images in the first row were taken at x400 total magnification and display the overview, while the images in the second row were taken at x1000 total magnification using immersion oil and show a close-up view of the cell in question.

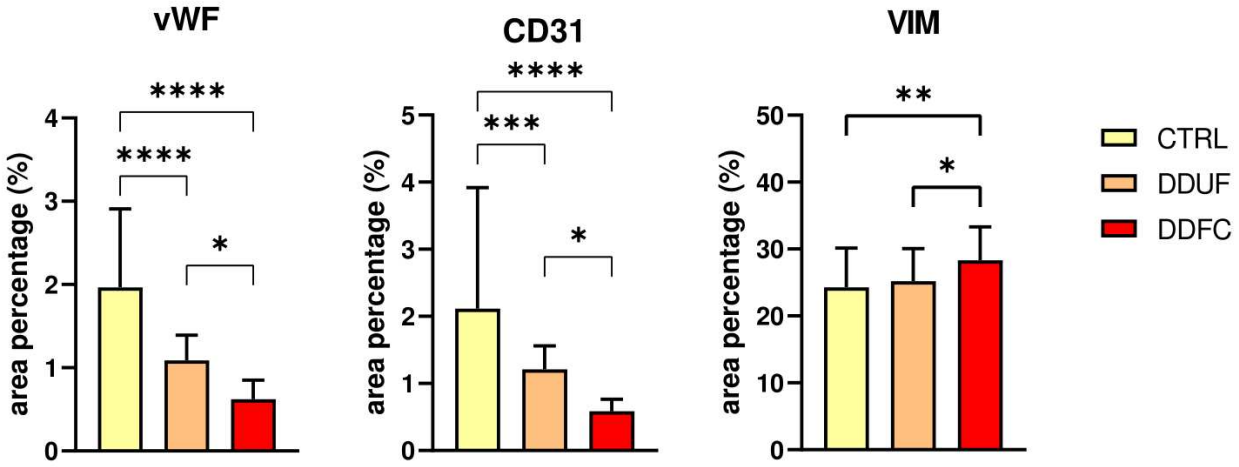

Figure 11. Bar graphs representing the expression of von Willebrand factor (vWF), cluster of differentiation 31 (CD31), and vimentin (VIM) in the analyzed samples. CTRL – palmar fascia of patients with carpal tunnel syndrome, DDUF - macroscopically unaffected palmar fascia from patients with Dupuytren's disease (DD), DDFC – fibrotic cords from patients with DD. The values are given as the means of the area percentage. Error bars represent the standard deviation. The statistical significance of differences was determined by two-way analysis of variance followed by Tukey's post hoc test. * $p < 0.05$; ** $p < 0.01$; *** $p < 0.001$; **** $p < 0.0001$.

We analyzed the samples to determine whether the EndoMT-related TF SNAI2 was expressed in endothelial cells (**Figure 12**). CD31 was used to confirm the endothelial phenotype of the cells. In CTRL samples, positive staining for SNAI2 was rarely present and it was mostly found in some connective tissue cells with a weak intensity. Contrary to this, both DDUF and DDFC samples contained endothelial cells with strong nuclear staining for SNAI2. Additionally, strong nuclear staining for SNAI2 could be observed in the surrounding connective tissue cells.

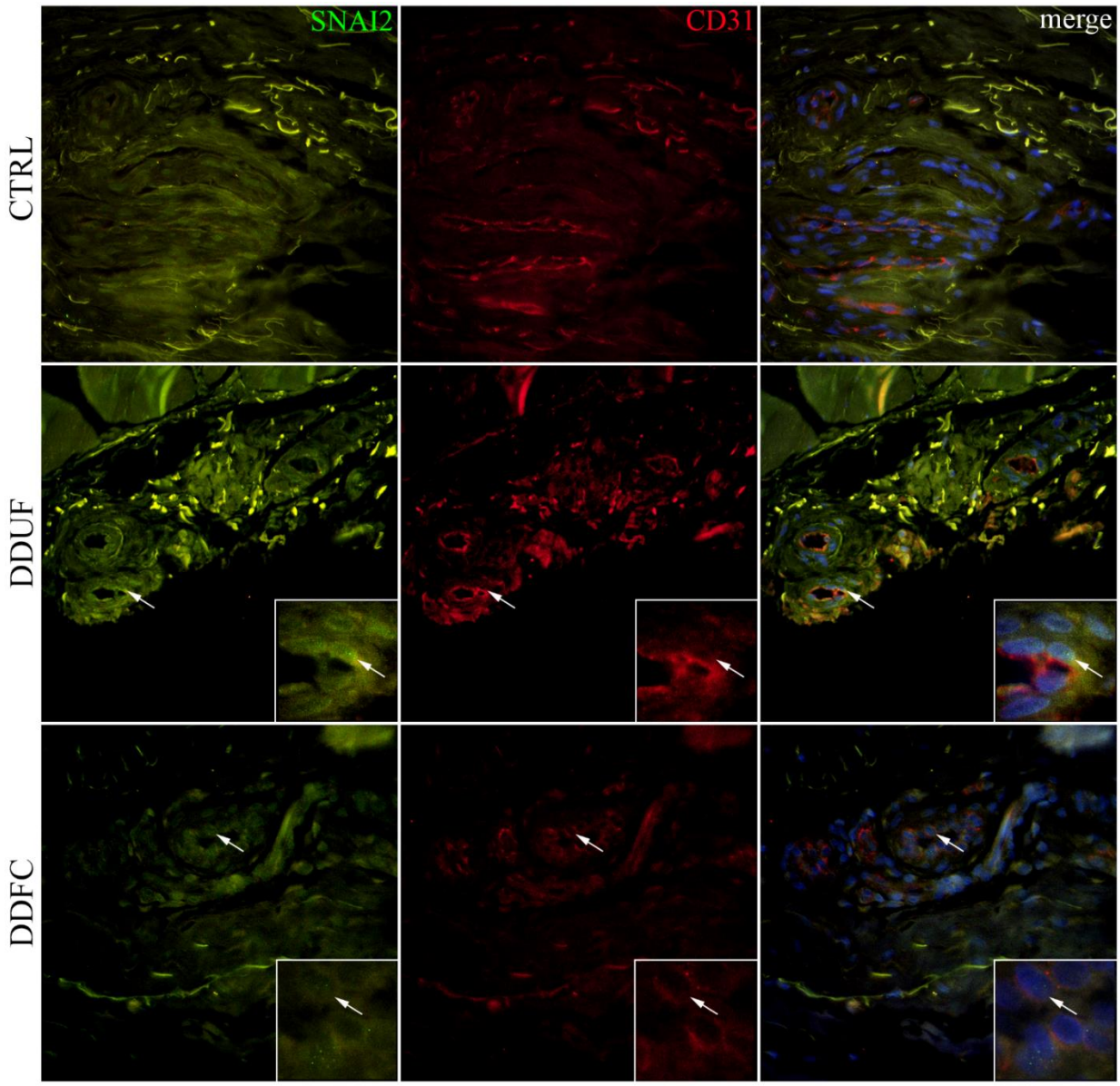

Figure 12. Expression of SNAI2 and cluster of differentiation 31 (CD31) in the analyzed samples. CTRL – palmar fascia of patients with carpal tunnel syndrome, DDUF - macroscopically unaffected palmar fascia from patients with Dupuytren's disease (DD), DDFC – fibrotic cords from patients with DD. The first panels (green signal) represent the staining for SNAI2, while the second panels (red signal) represent CD31 staining. The third panels represent the first two panels merged together with the nuclear staining (blue signal). Arrows mark endothelial cells positive for SNAI2 and CD31. The main images were taken at x400 total magnification, while the insets found in the bottom right of the panels were taken at x1000 total magnification using immersion oil.

5. DISCUSSION

Our study investigated the occurrence of EndoMT in DD by analyzing the expression of endothelial and mesenchymal markers, and the EndoMT-related transcription factor SNAI2 in palmar fascia samples from DD patients and healthy controls. Using immunofluorescence staining and quantitative analysis, we found significant reductions in endothelial markers (vWF and CD31) and increased expression of the mesenchymal marker vimentin in the endothelial cells of DD samples. Additionally, SNAI2 was upregulated in these cells, suggesting active EndoMT.

Recent investigations have demonstrated the involvement of EMT of sweat gland cells in the pathogenesis of DD. Cardenas-Leon *et al*. have identified colocalization of β-catenin with αSMA and vimentin in the sweat glands of DD patients but not in normal controls. Their study further reported downregulation of epithelial markers E-cadherin, α-catenin, β-catenin, and p120, alongside expression of connective tissue growth factor (CTGF) in the sweat glands of DD patients (111, 112). CTGF is known to act in an autocrine manner, inducing TGF-β and promoting EMT, or through paracrine mechanisms, facilitating myofibroblast differentiation (113). These findings align with previous research demonstrating the involvement of EMT of sweat glands in fibrosis among morphea patients (95).

Tripkovic *et al.* further elucidated the role of CTGF in DD, showing increased expression in blood vessels and connective tissue cells in palmar fascia samples of DD patients (114). This further supports the influence of CTGF on EMT and subsequent fibrosis in DD, consistent with observations in the sweat glands of DD patients reported by Cardenas-Leon *et al*. (111). The presence of increased CTGF expression in the endothelium of DD patients could act as an inducer of EndoMT. Furthermore, FGFR1 expression has been demonstrated to repress EndoMT (103, 115). Tripkovic *et al*. observed higher FGFR1 expression in macroscopically unaffected fascia compared to fibrotic cords in DD patients (114). This is in line with our results that show increased EndoMT-associated changes in the fibrotic cords compared to the macroscopically unaffected fascia of DD patients.

The origin of myofibroblasts, central to wound healing and fibrosis, remains complex and multifaceted. Myofibroblasts were thought to derive primarily from resident fibroblasts; however, recent evidence reveals additional sources including pericytes, bone marrow-derived fibrocytes, and cells undergoing transition processes such as EMT and EndoMT (116, 117). In renal fibrosis, myofibroblasts predominantly arise from local proliferation of resident fibroblasts (approximately 50%) and bone marrow progenitors (35%), with smaller

contributions from the EMT (5%) and EndoMT (10%) processes (118). The absence of robust, widely usable animal models for DD hinders precise lineage tracing of myofibroblast origins, making such specific results unlikely as of now (119). These findings however underscore the need for innovative research methodologies to determine myofibroblast origins and to form therapeutic strategies aimed at mitigating fibrosis by targeting specific cellular pathways involved in EMT and EndoMT. Targeting EndoMT may present a promising therapeutic approach for fibrotic diseases. Several pharmacological agents, such as ponatinib and imatinib, have demonstrated efficacy in preclinical models by attenuating EndoMT through modulation of signaling pathways (120, 121). Similarly, losartan and relaxin have shown potential in suppressing EndoMT and mitigating cardiac fibrosis (122, 123), while medications such as vildagliptin reduce lung fibrosis by inhibiting EndoMT (124).

Interestingly, we observed that these cellular changes typical for EndoMT are detectable even in macroscopically unaffected fascia. This observation extends on previous findings of macroscopically normal DD fascia being abnormal on both a histologic and molecular level (114, 125), by suggesting that fibrotic changes, in this case EndoMT, begin microscopically prior to clinical manifestations. This subclinical pathology likely contributes to the higher recurrence rates seen in less invasive surgical therapies, as even macroscopically unaffected fascia could provide a reservoir for pathogenic cells. The presence of EndoMT in seemingly normal fascia could explain the persistence and recurrence of fibrosis post-surgery, with endothelial cells perpetuating the fibrotic process by undergoing EndoMT.

Our study has limitations that warrant consideration. The sample size was limited and the research was conducted at a single center, which may affect the generalizability of our findings considering that the degree of fibrosis is not always uniform in DD. The absence of robust animal models for DD excludes accurate lineage tracing of epithelial and endothelial cells. Also, formal quantification of the expression of endothelial and mesenchymal markers via Western blotting or flow cytometry could not be performed as the samples used were formalin-fixed and paraffin-embedded.

Despite these limitations, the demonstration of EndoMT in DD has significant therapeutic implications. Targeting the pathways that regulate EndoMT could offer novel approaches to mitigate fibrosis in DD. Inhibitors of key signaling molecules and pathways may prove effective in reducing myofibroblast formation and subsequent fibrosis. Additionally, therapeutic strategies aimed at maintaining endothelial cell identity or preventing their

transition to mesenchymal states could emerge as potential treatments for DD and other fibrotic conditions. Lastly, due to the subclinical pathology in seemingly normal fascia, more extensive surgery, if tolerable by patients, may be preferred in the future.

6. CONCLUSIONS

1. The expression of the endothelial markers vWF and CD31 is decreased in the endothelial cells of the palmar fascia of patients with DD compared to healthy palmar fascia tissue.

2. The expression of the mesenchymal marker vimentin is increased in the endothelial cells of the palmar fascia of patients with DD compared to healthy palmar fascia tissue.

3. The EndoMT-related TF SNAI2 is expressed in the endothelial cells of the palmar fascia of patients with DD.

4. Both the fibrotic cords and the adjacent macroscopically unaffected palmar fascia of patients with DD demonstrate changes in protein expression associated with EndoMT.

5. The changes in protein expression associated with EndoMT are more extensive in the fibrotic cords than the adjacent macroscopically unaffected palmar fascia of patients with DD.

6. EndoMT is present and probably contributes to the fibrosis in DD, both in the early and late stages of pathogenesis.

7. A more extensive excision of palmar fascia during surgical treatment could lead to a lower recurrence rate of DD.

7. REFERENCES

1. Trumble TE, Rayan GM, Budoff JE, Baratz ME, Slutsky DJ. Principles of hand surgery and therapy. 3rd ed. Philadelphia: Elsevier; 2016. 840 p.
2. McGrouther DA. The microanatomy of Dupuytren's contracture. Hand. 1982;14:215-36.
3. Bilderback KK, Rayan GM. The septa of Legueu and Juvara: an anatomic study. J Hand Surg Am. 2004;29:494-9.
4. Gosset J. Dupuytren's disease and the anatomy of the palmodigital aponeurosis. In: Hueston JT, Tubiana R, editors. Dupuytren's disease. 2nd ed. Edinburgh: Churchill Livingstone; 1985. p. 13-6.
5. Thomine JM. The development and anatomy of the digital fascia. In: Hueston JT, Tubiana R, editors. Dupuytren's disease. Edinburgh: Churchill Livingstone; 1985. p. 3-12.
6. Luck JV. Dupuytren's contracture; a new concept of the pathogenesis correlated with surgical management. J Bone Joint Surg Am. 1959;41:635-64.
7. Shih B, Brown JJ, Armstrong DJ, Lindau T, Bayat A. Differential gene expression analysis of subcutaneous fat, fascia, and skin overlying a Dupuytren's disease nodule in comparison to control tissue. Hand (N Y). 2009;4:294-301.
8. Larsen S, Krogsgaard DG, Aagaard Larsen L, Iachina M, Skytthe A, Frederiksen H. Genetic and environmental influences in Dupuytren's disease: a study of 30,330 Danish twin pairs. J Hand Surg Eur Vol. 2015;40:171-6.
9. McFarlane RM. Patterns of the diseased fascia in the fingers in Dupuytren's contracture. Displacement of the neurovascular bundle. Plast Reconstr Surg. 1974;54:31-44.
10. Wilburn J, McKenna SP, Perry-Hinsley D, Bayat A. The impact of Dupuytren disease on patient activity and quality of life. J Hand Surg Am. 2013;38:1209-14.
11. Zerajic D, Finsen V. Dupuytren's disease in Bosnia and Herzegovina. An epidemiological study. BMC Musculoskelet Disord. 2004;5:10.
12. Salari N, Heydari M, Hassanabadi M, Kazeminia M, Farshchian N, Niaparast M, et al. The worldwide prevalence of the Dupuytren disease: a comprehensive systematic review and meta-analysis. J Orthop Surg Res. 2020;15:495.
13. Nordenskjold J, Englund M, Zhou C, Atroshi I. Prevalence and incidence of doctor-diagnosed Dupuytren's disease: a population-based study. J Hand Surg Eur Vol. 2017;42:673-7.
14. Al-Qattan MM. Factors in the pathogenesis of Dupuytren's contracture. J Hand Surg Am. 2006;31:1527-34.

15. Anthony SG, Lozano-Calderon SA, Simmons BP, Jupiter JB. Gender ratio of Dupuytren's disease in the modern U.S. population. Hand (N Y). 2008;3:87-90.
16. McFarlane RM, McGrouther DA, Flint MH. Dupuytren's disease biology and treatment. Edinburgh: Churchill Livingstone; 1990. 451 p.
17. Rayan GM, Moore J. Non-Dupuytren's disease of the palmar fascia. J Hand Surg Br. 2005;30:551-6.
18. Riesmeijer SA, Kamali Z, Ng M, Drichel D, Piersma B, Becker K, et al. A genome-wide association meta-analysis implicates Hedgehog and Notch signaling in Dupuytren's disease. Nat Commun. 2024;15:199.
19. Broekstra DC, Groen H, Molenkamp S, Werker PMN, van den Heuvel ER. A Systematic Review and Meta-Analysis on the Strength and Consistency of the Associations between Dupuytren Disease and Diabetes Mellitus, Liver Disease, and Epilepsy. Plast Reconstr Surg. 2018;141:367e-79e.
20. Descatha A, Jauffret P, Chastang JF, Roquelaure Y, Leclerc A. Should we consider Dupuytren's contracture as work-related? A review and meta-analysis of an old debate. BMC Musculoskelet Disord. 2011;12:96.
21. Wang Z, Yan Z, Xu Z, Gao A. Smoking, alcohol consumption and risk of Dupuytren's disease: a Mendelian randomization study. BMC Med Genomics. 2023;16:212.
22. Das SK, Vasudevan DM. Alcohol-induced oxidative stress. Life Sci. 2007;81:177-87.
23. Driver J, Weber CE, Callaci JJ, Kothari AN, Zapf MA, Roper PM, et al. Alcohol inhibits osteopontin-dependent transforming growth factor-beta1 expression in human mesenchymal stem cells. J Biol Chem. 2015;290:9959-73.
24. Ranzer MJ, Chen L, DiPietro LA. Fibroblast function and wound breaking strength is impaired by acute ethanol intoxication. Alcohol Clin Exp Res. 2011;35:83-90.
25. Ng M, Lawson DJ, Winney B, Furniss D. Is Dupuytren's disease really a 'disease of the Vikings'? J Hand Surg Eur Vol. 2020;45:273-9.
26. Burge P. Genetics of Dupuytren's disease. Hand Clin. 1999;15:63-71.
27. Bayat A, Walter J, Lambe H, Watson JS, Stanley JK, Marino M, et al. Identification of a novel mitochondrial mutation in Dupuytren's disease using multiplex DHPLC. Plast Reconstr Surg. 2005;115:134-41.
28. Alser OH, Kuo RYL, Furniss D. Nongenetic Factors Associated with Dupuytren's Disease: A Systematic Review. Plast Reconstr Surg. 2020;146:799-807.

29. Pagnotta A, Specchia N, Soccetti A, Manzotti S, Greco F. Responsiveness of Dupuytren's disease fibroblasts to 5 alpha-dihydrotestosterone. J Hand Surg Am. 2003;28:1029-34.

30. Baird KS, Crossan JF, Ralston SH. Abnormal growth factor and cytokine expression in Dupuytren's contracture. J Clin Pathol. 1993;46:425-8.

31. Badalamente MA, Hurst LC. The biochemistry of Dupuytren's disease. Hand Clin. 1999;15:35-42.

32. Qureshi FI, Hornigold R, Spencer JD, Hall SM. Langerhans cells in Dupuytren's contracture. J Hand Surg Br. 2001;26:362-7.

33. Fitzgerald AM, Kirkpatrick JJ, Foo IT, Naylor IL. A picropolychrome staining technique applied to Dupuytren's tissue. J Hand Surg Br. 1995;20:519-24.

34. Plewes LW. Sudeck's atrophy in the hand. J Bone Joint Surg Br. 1956;38:195-203.

35. Murrell GA, Francis MJ, Howlett CR. Dupuytren's contracture. Fine structure in relation to aetiology. J Bone Joint Surg Br. 1989;71:367-73.

36. Rayan GM, Parizi M, Tomasek JJ. Pharmacologic regulation of Dupuytren's fibroblast contraction in vitro. J Hand Surg Am. 1996;21:1065-70.

37. Bazin S, Le Lous M, Duance VC, Sims TJ, Bailey AJ, Gabbiani G, et al. Biochemistry and histology of the connective tissue of Dupuytren's disease lesions. Eur J Clin Invest. 1980;10:9-16.

38. Murrell GA, Francis MJ, Bromley L. The collagen changes of Dupuytren's contracture. J Hand Surg Br. 1991;16:263-6.

39. Ulrich D, Hrynyschyn K, Pallua N. Matrix metalloproteinases and tissue inhibitors of metalloproteinases in sera and tissue of patients with Dupuytren's disease. Plast Reconstr Surg. 2003;112:1279-86.

40. Tomasek JJ, Haaksma CJ. Fibronectin filaments and actin microfilaments are organized into a fibronexus in Dupuytren's diseased tissue. Anat Rec. 1991;230:175-82.

41. Tomasek J, Rayan GM. Correlation of alpha-smooth muscle actin expression and contraction in Dupuytren's disease fibroblasts. J Hand Surg Am. 1995;20:450-5.

42. Akhavani MA, McMurtrie A, Webb M, Muir L. A review of the classification of Dupuytren's disease. J Hand Surg Eur Vol. 2015;40:155-65.

43. Rayan GM. Dupuytren disease: Anatomy, pathology, presentation, and treatment. J Bone Joint Surg Am. 2007;89:189-98.

44. Rayan GM, Ali M, Orozco J. Dorsal pads versus nodules in normal population and Dupuytren's disease patients. J Hand Surg Am. 2010;35:1571-9.

45. Flint MH. The genesis of the palmar lesion. In: McFarlane RM, McGrouther DA, Flint MH, editors. Dupuytren's disease biology and treatment. Edinburgh: Churchill Livingstone; 1990. p. 136-54.
46. Loos B, Puschkin V, Horch RE. 50 years experience with Dupuytren's contracture in the Erlangen University Hospital--a retrospective analysis of 2919 operated hands from 1956 to 2006. BMC Musculoskelet Disord. 2007;8:60.
47. Dutta A, Jayasinghe G, Deore S, Wahed K, Bhan K, Bakti N, et al. Dupuytren's Contracture - Current Concepts. J Clin Orthop Trauma. 2020;11:590-6.
48. Townley WA, Baker R, Sheppard N, Grobbelaar AO. Dupuytren's contracture unfolded. BMJ. 2006;332:397-400.
49. Ng AWH, Griffith JF, Ng ISH. MRI of carpal tunnel syndrome: before and after carpal tunnel release. Clin Radiol. 2021;76:940 e29- e35.
50. Rombouts JJ, Noel H, Legrain Y, Munting E. Prediction of recurrence in the treatment of Dupuytren's disease: evaluation of a histologic classification. J Hand Surg Am. 1989;14:644-52.
51. Fernando JJ, Fowler C, Graham T, Terry K, Grocott P, Sandford F. Pre-operative hand therapy management of Dupuytren's disease: A systematic review. Hand Ther. 2024;29:52-61.
52. Aykut S, Aydin C, Ozturk K, Arslanoglu F, Kilinc CY. Extracorporeal Shock Wave Therapy in Dupuytren's Disease. Sisli Etfal Hastan Tip Bul. 2018;52:124-8.
53. Brunelli S, Bonanni C, Traballesi M, Foti C. Radial extracorporeal shock wave therapy: a novel approach for the treatment of Dupuytren's contractures: A case report. Medicine (Baltimore). 2020;99:e20587.
54. Notarnicola A, Maccagnano G, Rifino F, Pesce V, Gallone MF, Covelli I, et al. Short-term effect of shockwave therapy, temperature controlled high energy adjustable multi-mode emission laser or stretching in Dupuytren's disease: a prospective randomized clinical trial. J Biol Regul Homeost Agents. 2017;31:775-84.
55. McCarthy DM. The long-term results of enzymic fasciotomy. J Hand Surg Br. 1992;17:356.
56. Ketchum LD, Donahue TK. The injection of nodules of Dupuytren's disease with triamcinolone acetonide. J Hand Surg Am. 2000;25:1157-62.
57. Steppe C, Cinclair R, Lies S. A 10-Year Review of Collagenase Versus Fasciectomy in the Treatment of Dupuytren Contracture. Ann Plast Surg. 2024;92:642-6.

58. Betz N, Ott OJ, Adamietz B, Sauer R, Fietkau R, Keilholz L. Radiotherapy in early-stage Dupuytren's contracture. Long-term results after 13 years. Strahlenther Onkol. 2010;186:82-90.
59. Clibbon JJ, Logan AM. Palmar segmental aponeurectomy for Dupuytren's disease with metacarpophalangeal flexion contracture. J Hand Surg Br. 2001;26:360-1.
60. Jurisic D, Kovic I, Lulic I, Stanec Z, Kapovic M, Uravic M. Dupuytren's disease characteristics in Primorsko-goranska County, Croatia. Coll Antropol. 2008;32:1209-13.
61. Ashdown T, Hayter E, Morris JA, Clough OT, Little M, Hardman J, et al. Repeat limited fasciectomy is a safe and effective treatment for recurrence of Dupuytren's disease. Bone Joint J. 2021;103:946-50.
62. Moermans JP. Long-term results after segmental aponeurectomy for Dupuytren's disease. J Hand Surg Br. 1996;21:797-800.
63. Chick LR, Lister GD. Surgical alternatives in Dupuytren's contracture. Hand Clin. 1991;7:715-9
64. McCash CR. The Open Palm Technique in Dupuytren's Contracture. Br J Plast Surg. 1964;17:271-80.
65. Ketchum LD. Expanded Dermofasciectomies and Full-Thickness Grafts in the Treatment of Dupuytren’s Contracture: A 36-Year Experience. In: Eaton C, Seegenschmiedt MH, Bayat A, Gabbiani G, Werker P, Wach W, editors. Dupuytren’s disease and related hyperproliferative disorders. Heidelberg: Springer Berlin; 2012. p. 213-20.
66. van Rijssen AL, Gerbrandy FS, Ter Linden H, Klip H, Werker PM. A comparison of the direct outcomes of percutaneous needle fasciotomy and limited fasciectomy for Dupuytren's disease: a 6-week follow-up study. J Hand Surg Am. 2006;31:717-25.
67. van Rijssen AL, Ter Linden H, Werker PMN. Five-year results of a randomized clinical trial on treatment in Dupuytren's disease: percutaneous needle fasciotomy versus limited fasciectomy. Plast Reconstr Surg. 2012;129:469-77.
68. Karam M, Kahlar N, Abul A, Rahman S, Pinder R. Comparison of Hand Therapy with or without Splinting Postfasciectomy for Dupuytren's Contracture: Systematic Review and Meta-Analysis. J Hand Microsurg. 2022;14:308-14.
69. Debnath P, Huirem RS, Dutta P, Palchaudhuri S. Epithelial-mesenchymal transition and its transcription factors. Biosci Rep. 2022;42:BSR20211754.
70. Stemmler MP, Eccles RL, Brabletz S, Brabletz T. Non-redundant functions of EMT transcription factors. Nat Cell Biol. 2019;21:102-12.

71. Kalluri R, Weinberg RA. The basics of epithelial-mesenchymal transition. J Clin Invest. 2009;119:1420-8.
72. Francou A, Anderson KV. The Epithelial-to-Mesenchymal Transition (EMT) in Development and Cancer. Annu Rev Cancer Biol. 2020;4:197-220.
73. Gammill LS, Bronner-Fraser M. Neural crest specification: migrating into genomics. Nat Rev Neurosci. 2003;4:795-805.
74. Campbell K. Contribution of epithelial-mesenchymal transitions to organogenesis and cancer metastasis. Curr Opin Cell Biol. 2018;55:30-5.
75. Lopez-Novoa JM, Nieto MA. Inflammation and EMT: an alliance towards organ fibrosis and cancer progression. EMBO Mol Med. 2009;1:303-14.
76. Di Gregorio J, Robuffo I, Spalletta S, Giambuzzi G, De Iuliis V, Toniato E, et al. The Epithelial-to-Mesenchymal Transition as a Possible Therapeutic Target in Fibrotic Disorders. Front Cell Dev Biol. 2020;8:607483.
77. Gonzalez DM, Medici D. Signaling mechanisms of the epithelial-mesenchymal transition. Sci Signal. 2014;7:re8.
78. Sosa Pena MDP, Lopez-Soler R, Melendez JA. Senescence in chronic allograft nephropathy. Am J Physiol Renal Physiol. 2018;315:F880-F9.
79. Vigneron A, Vousden KH. p53, ROS and senescence in the control of aging. Aging (Albany NY). 2010;2:471-4.
80. Muthuramalingam K, Cho M, Kim Y. Cellular senescence and EMT crosstalk in bleomycin-induced pathogenesis of pulmonary fibrosis-an in vitro analysis. Cell Biol Int. 2020;44:477-87.
81. Yamaguchi M, Hirai S, Tanaka Y, Sumi T, Miyajima M, Mishina T, et al. Fibroblastic foci, covered with alveolar epithelia exhibiting epithelial-mesenchymal transition, destroy alveolar septa by disrupting blood flow in idiopathic pulmonary fibrosis. Lab Invest. 2017;97:232-42.
82. Yang ZC, Yi MJ, Ran N, Wang C, Fu P, Feng XY, et al. Transforming growth factor-beta1 induces bronchial epithelial cells to mesenchymal transition by activating the Snail pathway and promotes airway remodeling in asthma. Mol Med Rep. 2013;8:1663-8.
83. Zolak JS, Jagirdar R, Surolia R, Karki S, Oliva O, Hock T, et al. Pleural mesothelial cell differentiation and invasion in fibrogenic lung injury. Am J Pathol. 2013;182:1239-47.
84. Michelotti GA, Xie G, Swiderska M, Choi SS, Karaca G, Kruger L, et al. Smoothened is a master regulator of adult liver repair. J Clin Invest. 2013;123:2380-94.

85. Luo GH, Lu YP, Yang L, Song J, Shi YJ, Li YP. Epithelial to mesenchymal transformation in tubular epithelial cells undergoing anoxia. Transplant Proc. 2008;40:2800-3.
86. Grande MT, Sanchez-Laorden B, Lopez-Blau C, De Frutos CA, Boutet A, Arevalo M, et al. Snail1-induced partial epithelial-to-mesenchymal transition drives renal fibrosis in mice and can be targeted to reverse established disease. Nat Med. 2015;21:989-97.
87. Lovisa S, LeBleu VS, Tampe B, Sugimoto H, Vadnagara K, Carstens JL, et al. Epithelial-to-mesenchymal transition induces cell cycle arrest and parenchymal damage in renal fibrosis. Nat Med. 2015;21:998-1009.
88. Wang X, Gao Y, Tian N, Wang T, Shi Y, Xu J, et al. Astragaloside IV inhibits glucose-induced epithelial-mesenchymal transition of podocytes through autophagy enhancement via the SIRT-NF-kappaB p65 axis. Sci Rep. 2019;9:323.
89. Scharl M, Weber A, Furst A, Farkas S, Jehle E, Pesch T, et al. Potential role for SNAIL family transcription factors in the etiology of Crohn's disease-associated fistulae. Inflamm Bowel Dis. 2011;17:1907-16.
90. Kang DH. Loosening of the mesothelial barrier as an early therapeutic target to preserve peritoneal function in peritoneal dialysis. Kidney Res Clin Pract. 2020;39:136-44.
91. Blom JN, Feng Q. Cardiac repair by epicardial EMT: Current targets and a potential role for the primary cilium. Pharmacol Ther. 2018;186:114-29.
92. Duan J, Gherghe C, Liu D, Hamlett E, Srikantha L, Rodgers L, et al. Wnt1/betacatenin injury response activates the epicardium and cardiac fibroblasts to promote cardiac repair. EMBO J. 2012;31:429-42.
93. Du L, Hao M, Li C, Wu W, Wang W, Ma Z, et al. Quercetin inhibited epithelial mesenchymal transition in diabetic rats, high-glucose-cultured lens, and SRA01/04 cells through transforming growth factor-beta2/phosphoinositide 3-kinase/Akt pathway. Mol Cell Endocrinol. 2017;452:44-56.
94. Saika S, Yamanaka O, Flanders KC, Okada Y, Miyamoto T, Sumioka T, et al. Epithelial-mesenchymal transition as a therapeutic target for prevention of ocular tissue fibrosis. Endocr Metab Immune Disord Drug Targets. 2008;8:69-76.
95. Takahashi M, Akamatsu H, Yagami A, Hasegawa S, Ohgo S, Abe M, et al. Epithelial-mesenchymal transition of the eccrine glands is involved in skin fibrosis in morphea. J Dermatol. 2013;40:720-5.
96. Kuwahara H, Tosa M, Egawa S, Murakami M, Mohammad G, Ogawa R. Examination of Epithelial Mesenchymal Transition in Keloid Tissues and Possibility of Keloid Therapy Target. Plast Reconstr Surg Glob Open. 2016;4:e1138.

97. Hong L, Du X, Li W, Mao Y, Sun L, Li X. EndMT: A promising and controversial field. Eur J Cell Biol. 2018;97:493-500.
98. Eisenberg LM, Markwald RR. Molecular regulation of atrioventricular valvuloseptal morphogenesis. Circ Res. 1995;77:1-6.
99. Kokudo T, Suzuki Y, Yoshimatsu Y, Yamazaki T, Watabe T, Miyazono K. Snail is required for TGFbeta-induced endothelial-mesenchymal transition of embryonic stem cell-derived endothelial cells. J Cell Sci. 2008;121:3317-24.
100. Garside VC, Chang AC, Karsan A, Hoodless PA. Co-ordinating Notch, BMP, and TGF-beta signaling during heart valve development. Cell Mol Life Sci. 2013;70:2899-917.
101. Xiao L, Dudley AC. Fine-tuning vascular fate during endothelial-mesenchymal transition. J Pathol. 2017;241:25-35.
102. Chen PY, Qin L, Tellides G, Simons M. Fibroblast growth factor receptor 1 is a key inhibitor of TGFbeta signaling in the endothelium. Sci Signal. 2014;7:ra90.
103. Chen PY, Qin L, Barnes C, Charisse K, Yi T, Zhang X, et al. FGF regulates TGF-beta signaling and endothelial-to-mesenchymal transition via control of let-7 miRNA expression. Cell Rep. 2012;2:1684-96.
104. Widyantoro B, Emoto N, Nakayama K, Anggrahini DW, Adiarto S, Iwasa N, et al. Endothelial cell-derived endothelin-1 promotes cardiac fibrosis in diabetic hearts through stimulation of endothelial-to-mesenchymal transition. Circulation. 2010;121:2407-18.
105. Zeisberg EM, Tarnavski O, Zeisberg M, Dorfman AL, McMullen JR, Gustafsson E, et al. Endothelial-to-mesenchymal transition contributes to cardiac fibrosis. Nat Med. 2007;13:952-61.
106. Manetti M, Romano E, Rosa I, Guiducci S, Bellando-Randone S, De Paulis A, et al. Endothelial-to-mesenchymal transition contributes to endothelial dysfunction and dermal fibrosis in systemic sclerosis. Ann Rheum Dis. 2017;76:924-34.
107. Rosa I, Romano E, Fioretto BS, Manetti M. The contribution of mesenchymal transitions to the pathogenesis of systemic sclerosis. Eur J Rheumatol. 2020;7:S157-S64.
108. Manetti M, Guiducci S, Matucci-Cerinic M. The origin of the myofibroblast in fibroproliferative vasculopathy: does the endothelial cell steer the pathophysiology of systemic sclerosis? Arthritis Rheum. 2011;63:2164-7.
109. Piera-Velazquez S, Mendoza FA, Jimenez SA. Endothelial to Mesenchymal Transition (EndoMT) in the Pathogenesis of Human Fibrotic Diseases. J Clin Med. 2016;5:45.

110. Romano E, Rosa I, Fioretto BS, Matucci-Cerinic M, Manetti M. New Insights into Profibrotic Myofibroblast Formation in Systemic Sclerosis: When the Vascular Wall Becomes the Enemy. Life (Basel). 2021;11:610.
111. Cardenas-Leon CG, Maemets-Allas K, Klaas M, Maasalu K, Jaks V. Proteomic Analysis of Dupuytren's Contracture-Derived Sweat Glands Revealed the Synthesis of Connective Tissue Growth Factor and Initiation of Epithelial-Mesenchymal Transition as Major Pathogenetic Events. Int J Mol Sci. 2023;24:1081.
112. Viil J, Maasalu K, Maemets-Allas K, Tamming L, Lohmussaar K, Tooming M, et al. Laminin-rich blood vessels display activated growth factor signaling and act as the proliferation centers in Dupuytren's contracture. Arthritis Res Ther. 2015;17:144.
113. Sonnylal S, Xu S, Jones H, Tam A, Sreeram VR, Ponticos M, et al. Connective tissue growth factor causes EMT-like cell fate changes in vivo and in vitro. J Cell Sci. 2013;126:2164-75.
114. Tripkovic I, Ogorevc M, Vukovic D, Saraga-Babic M, Mardesic S. Fibrosis-Associated Signaling Molecules Are Differentially Expressed in Palmar Connective Tissues of Patients with Carpal Tunnel Syndrome and Dupuytren's Disease. Biomedicines. 2022;10:3214.
115. Li J, Shi S, Srivastava SP, Kitada M, Nagai T, Nitta K, et al. FGFR1 is critical for the anti-endothelial mesenchymal transition effect of N-acetyl-seryl-aspartyl-lysyl-proline via induction of the MAP4K4 pathway. Cell Death Dis. 2017;8:e2965.
116. Piera-Velazquez S, Li Z, Jimenez SA. Role of endothelial-mesenchymal transition (EndoMT) in the pathogenesis of fibrotic disorders. Am J Pathol. 2011;179:1074-80.
117. Hung CF. Origin of myofibroblasts in lung fibrosis. Curr Tissue Microenviron Rep. 2020;1:155-62.
118. LeBleu VS, Taduri G, O'Connell J, Teng Y, Cooke VG, Woda C, et al. Origin and function of myofibroblasts in kidney fibrosis. Nat Med. 2013;19:1047-53.
119. Satish L, Palmer B, Liu F, Papatheodorou L, Rigatti L, Baratz ME, et al. Developing an animal model of Dupuytren's disease by orthotopic transplantation of human fibroblasts into athymic rat. BMC Musculoskelet Disord. 2015;16:138.
120. Kang Z, Ji Y, Zhang G, Qu Y, Zhang L, Jiang W. Ponatinib attenuates experimental pulmonary arterial hypertension by modulating Wnt signaling and vasohibin-2/vasohibin-1. Life Sci. 2016;148:1-8.
121. Song S, Zhang M, Yi Z, Zhang H, Shen T, Yu X, et al. The role of PDGF-B/TGF-beta1/neprilysin network in regulating endothelial-to-mesenchymal transition in pulmonary artery remodeling. Cell Signal. 2016;28:1489-501.

122. Wylie-Sears J, Levine RA, Bischoff J. Losartan inhibits endothelial-to-mesenchymal transformation in mitral valve endothelial cells by blocking transforming growth factor-beta-induced phosphorylation of ERK. Biochem Biophys Res Commun. 2014;446:870-5.
123. Zhou X, Chen X, Cai JJ, Chen LZ, Gong YS, Wang LX, et al. Relaxin inhibits cardiac fibrosis and endothelial-mesenchymal transition via the Notch pathway. Drug Des Devel Ther. 2015;9:4599-611.
124. Suzuki T, Tada Y, Gladson S, Nishimura R, Shimomura I, Karasawa S, et al. Vildagliptin ameliorates pulmonary fibrosis in lipopolysaccharide-induced lung injury by inhibiting endothelial-to-mesenchymal transition. Respir Res. 2017;18:177.
125. Alfonso-Rodriguez CA, Garzon I, Garrido-Gomez J, Oliveira AC, Martin-Piedra MA, Scionti G, et al. Identification of histological patterns in clinically affected and unaffected palm regions in dupuytren's disease. PLoS One. 2014;9:e112457.

8. SUMMARY

Objectives: Our study aimed to investigate whether EndoMT contributes to fibrosis in DD by analyzing the expression of endothelial and mesenchymal markers, as well as an EndoMT-related TF, in the palmar fascia of DD patients and healthy fascia. We hypothesized that in DD patients, the endothelial cells of the palmar fascia would exhibit decreased expression of endothelial markers and increased expression of mesenchymal markers and the EndoMT-related TF.

Material and methods: Palmar fascia samples were collected from patients with DD and carpal tunnel syndrome, after which they were processed through fixation, dehydration, paraffin embedding, and sectioned for histological and immunofluorescence analyses. Hematoxylin and eosin staining, along with immunofluorescence staining for endothelial and mesenchymal markers, were performed on these sections, followed by digital image analysis to quantify the fluorescent signal. Two-way ANOVA with Tukey's post hoc test was used to assess for statistically significant differences in protein expression between sample groups.

Results: Immunofluorescence analysis revealed that the expressions of endothelial markers vWF and CD31 were significantly decreased, while the expressions of the mesenchymal marker vimentin and EndoMT-related TF SNAI2 were significantly increased in the endothelial cells of samples obtained from patients with DD compared to healthy controls. These changes were observed in both fibrotic cords and adjacent macroscopically unaffected palmar fascia, with more pronounced alterations in fibrotic cords. Statistical analyses confirmed that the observed differences in protein expression between sample groups were significant.

Conclusions: Considering the downregulation of endothelial markers, upregulation of mesenchymal markers and the expression of SNAI2, EndoMT is likely present and contributes to the fibrosis in the palmar fascia of DD patients. These changes were also found, albeit to a lesser degree, in macroscopically unaffected fascia, indicating that EndoMT occurs there as well. The presence of EndoMT in macroscopically unaffected fascia could explain the higher recurrence rates in less extensive surgical procedures and therapies targeting EndoMT could reduce clinical recurrences.

9. CROATIAN SUMMARY

Naslov: Endotelno-mezenhimska tranzicija u Dupuytrenovoj kontrakturi

Ciljevi: Cilj našeg istraživanja bio je odrediti doprinosi li endotelno-mezenhimska tranzicija (EndoMT) fibrozi u Dupuytrenovoj kontrakturi (DD) putem analize izražaja endotelnih i mezenhimalnih biljega te transkripcijskog čimbenika (TF) povezanog s EndoMT-om u palmarnoj fasciji bolesnika s DD-om i zdravoj fasciji. Naša hipoteza je da će u bolesnika s DD-om endotelne stanice palmarne fascije pokazivati smanjen izražaj endotelnih biljega i povećan izražaj mezenhimalnih biljega i TF-a povezanog s EndoMT-om.

Materijali i metode: Uzorci palmarne fascije prikupljeni su od bolesnika s DD-om i sindromom karpalnog tunela, nakon čega su fiksirani, dehidrirani i uklopljeni u parafin te izrađeni su rezovi za histološke i imunofluorescencijske analize. Bojenje hematoksilinom i eozinom, zajedno s imunofluorescencijskim bojenjem na endotelne i mezenhimalne biljege, provedeno je na ovim rezovima, nakon čega je uslijedila digitalna analiza slika za kvantificiranje fluorescentnog signala. Dvosmjerna analiza varijance s Tukeyjevim post hoc testom korištena je za procjenu statističke značajnosti razlika u izražaju proteina između skupina uzoraka.

Rezultati: Imunofluorescencijska analiza otkrila je da je izražaj endotelnih biljega von Willebrandovog čimbenika i klastera diferencijacije 31 značajno smanjen, dok je izražaj mezenhimalnog biljega vimentina i TF-a SNAI2 povezanog s EndoMT-om značajno povećan u endotelnim stanicama uzoraka bolesnika s DD-om u usporedbi sa zdravim kontrolama. Ove promjene uočene su i u fibroznim vrpcama i u okolnoj makroskopski nezahvaćenoj palmarnoj fasciji, s izraženijim promjenama u fibroznim vrpcama. Statističke analize potvrdile su značajnost opaženih razlika u izražaju proteina između skupina uzoraka.

Zaključci: Uzimajući u obzir smanjenje endotelnih biljega, povišenje mezenhimalnih biljega i izražaj SNAI2, EndoMT je vjerojatno prisutna i doprinosi fibrozi u palmarnoj fasciji bolesnika s DD-om. Ove promjene su također pronađene, iako u manjem rasponu, u makroskopski nezahvaćenoj fasciji, što ukazuje na to da se EndoMT također zbiva u tom tkivu. Prisutnost EndoMT-e u makroskopski nezahvaćenoj fasciji mogla bi objasniti veće stope recidiva kod primjene manje opsežnih kirurških zahvata, dok bi liječenje usmjereno na EndoMT-u moglo dovesti do smanjenja kliničkih recidiva.